Supporting information for

Exploration of anion effects in solvothermal synthesis using *in situ* X-ray diffraction

Contents

S1 Details on Rietveld refinements

All Rietveld refinements were performed with the FullProf software package using the Thompson-Cox-Hastings Pseudo Voigt peak shape formulation. One or two of the peak broadening parameters U, I_G, X, or Y were employed to provide the best description while keeping the model robust (with few refinable parameters) to cater the demands of the sequential refinements. Some phases or experimental time regions were challenging due to poor powder rings (*e.g.* presence of a few reflections from single crystals), existence of several phases with possible peak overlap or very weak signal. Here, the model was refined against one of the better diffractograms, in some cases with manually determined broadening parameters, but only allowed to refine scale factor, unit cell parameters, and background parameters during the sequential refinements.

The background was refined using linear interpolation between manually selected points. These were only assigned to regions without reflections to avoid false Bragg peak descriptions.

Due to the limited data quality and wide temperature range, isotropic B-values for all atoms were fixed at 0.8 $Å^2$ apart from CuI where a value of 2.8 $Å^2$ was used to account for the abnormal scattering from the disordered structure (iodine forms a ionic liquid sublattice at elevated temperature). Likewise the occupancies of atomic sites wasnot refined with the exemption of O and Cl in $MnCl_{0.7}(OH)_{1.3}$ (discussed in detail in S3).

Since high energy X-ray radiation was employed, appropriate scattering factors for all elements were looked up and used throughout the refinements.

To account for instrumental broadening, diffractograms on LaB_6 calibrants (NIST 660b) were measured and refined to obtain instrumental resolution files (irf), which were used across the *in situ* experiments. Obs-calc diagrams of the refined calibrants are plotted below, with observed data points in red, the modelled diffractogram in black and the difference curve in blue. Broadening parameters in the Thompson-Cox-Hastings Pseudo Voigt formalism are provided for each calibrant.

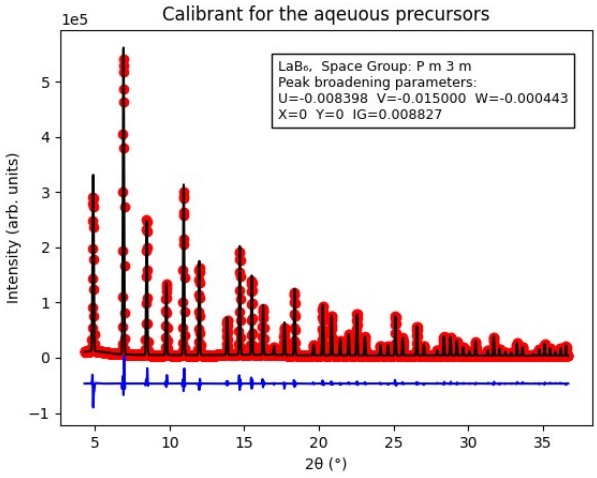

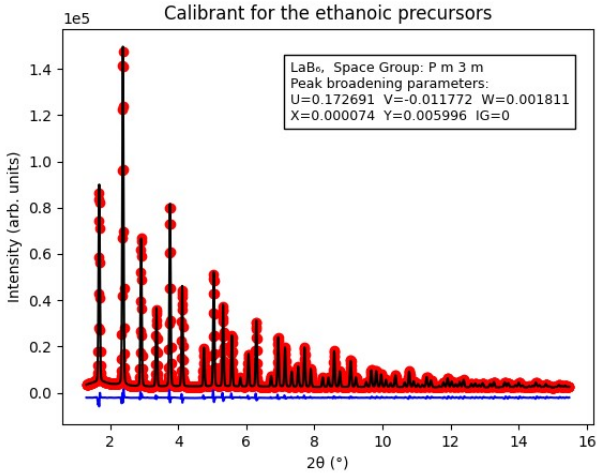

S2 Metal hydroxide sheet structures

Prior to the crystallization of CoO, distinct peaks were observed to emerge in the experiments with $Co(acac)_2$ and $Co(ace)_2{\cdot}4H_2O$. These peaks were assigned to sheets of $Co(OH)_2$ in space group P-3m1 based on the matching positions of all hk0 reflections, as it can be seen from Figure S2-1 (a).

The structure of $Co(OH)_2$ is layered in nature and consists of sheets of octahedrally coordinated Co^{2+} and 3-coordinated bridging hydroxyl groups Figure S2-1 (b). Since the formation of $Co(OH)_2$ sheets is limited to the precursors containing acetate or acetylacetonate one could speculate that these anions play a role in forming and/or stabilizing the sheets. It appears plausible that some of the hydroxyl ligands are replaced although the specific bonding and orientation of acetate or acetylacetonate is not obvious in such case. The difference in anion size would decrease the strength of the interlayer interactions and thus favor the presence of individual sheets. It should be emphasized that this is speculation and that solid experimental proof is necessary to determine the role of the anions.

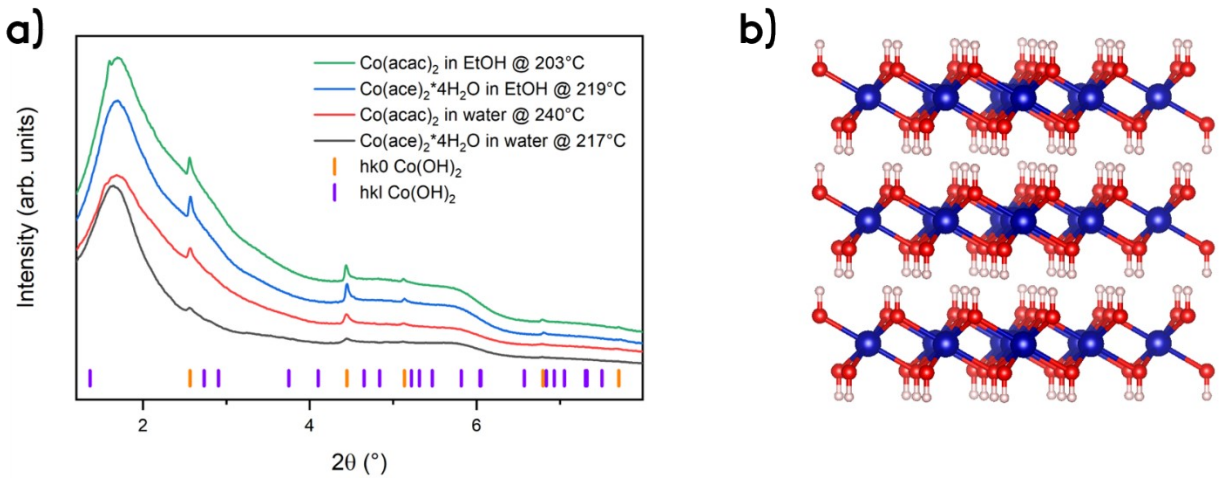

Figure S2-1. Diffractograms showing peaks from the phase labelled "$Co(OH)_2$ sheets" along with positions of reflections with and without an l component for $Co(OH)_2$ in space group P -3 m 1 (a) and an illustration of the atomic structure of the same phase (b).

For one sample, $Co(ace)_2{\cdot}4H_2O$ in ethanol, all reflections from $Co(OH)_2$ were found to emerge after a period of increasing intensity from the sheets-reflections (Figure S2-1). This indicates condensation and "full" crystallization into the 3D structure, and occurred simultaneously with the phase transition to CoO. The obs-calc diagram for the two-phase refinement of $Mn(OH)_2$ sheets (P-3m1) and Mn_3O_4 can be found in S5.34.

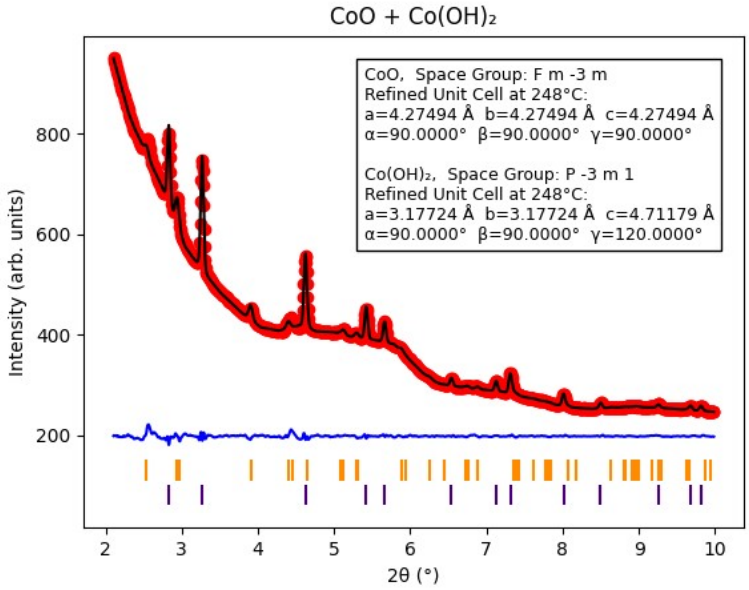

Figure S2-1. Obs-calc diagram for the two-phase refinement of CoO and $Co(OH)_2$ that have crystallized from $Co(ace)_2{\cdot}4H_2O$ in ethanol. The orange lines mark the positions of reflections from $Co(OH)_2$ and the indigo lines mark the positions of reflections from CoO.

S3 Manganese chloride hydroxide structures

Three phases were observed to crystallize from the ethanolic precursor of $MnCl_2{\cdot}4H_2O$ at high temperature (S5.15) and redissolve again. The peak positions of phase 1 and phase 3 were found to match those of two polymorphs of $FeCl_2$ (mineral name Lawrencite, both in space group R-3m) with the chloride ions stacking on top or in between interlayer ions, respectively. However, the relative intensities of reflections did not match the diffractograms for both phases. The stacking faulted $NiCl_2$ – $Ni(OH)_2$ (R-3m) shares the structural motif with one of the $FeCl_2$ polymorphs and served as isostructure for the refinement of $MnCl_{0.7}OH_{1.3}$. Visual representations of the structures are given in Figure S2-1.

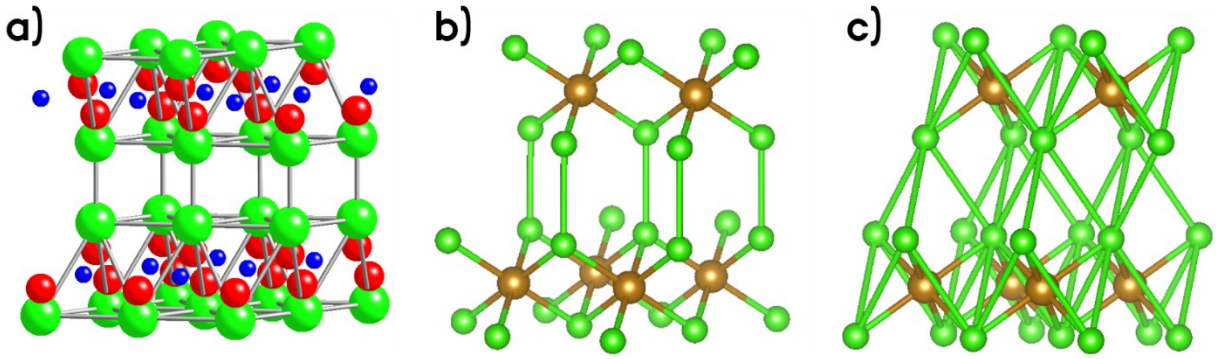

Figure S2-1. Structural models of $NiCl_2$ – $Ni(OH)_2$ (a) and $FeCl_2$ (lawrencite) with on top stacking (b) and in between stacking (c).

The occupancies of O and Cl were refined to determine the stoichiometry of $MnCl_{0.7}OH_{1.3}$ (but locked during sequential refinements for robustness). The unit cell parameters were refined to a = 3.496(2) Å and c = 17.42(4) Å compared to the reported values of a = 3.261 Å and 17.01 Å for $NiCl_2$ – $Ni(OH)_2$. Both the difference in anion size and the high temperature cause expansion of the unit cell.

The reflections from the third phase are only present in a narrow temperature region and together with trace reflections from the second phase. Furthermore, the detector images contain single crystal spots, meaning that the relative peak intensities are not reliable. For these reasons further, more detailed, modelling were not attempted. The obs-calc diagrams of the refinements of $MnCl_{0.7}OH_{1.3}$ (a) and the $FeCl_2$ isostructure $MnCl_2$ (b) against phase 1 are plotted in Figure S2-2 together with the other $FeCl_2$ isostructure $MnCl_2$ (c) refined against phase 3. Phase 2 could not be identified but is likely a manganese chloride

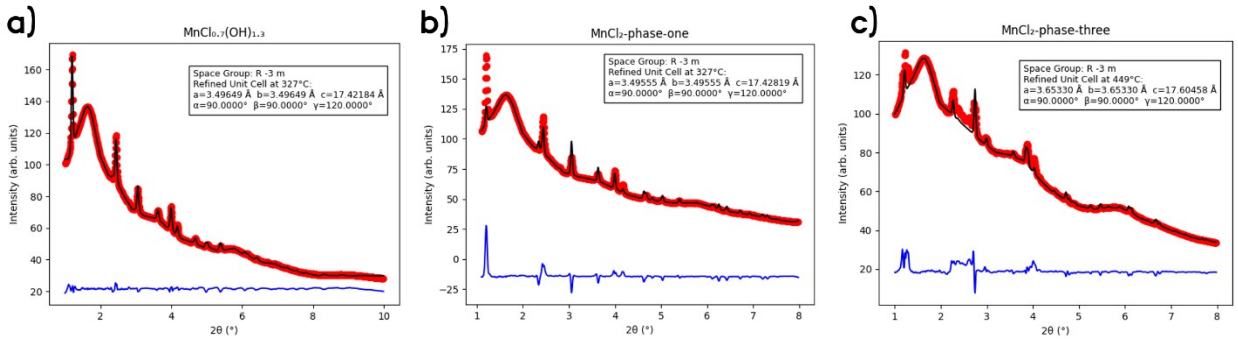

hydroxide with some structural distortions compared to the preceding and following phases.

Figure S2-2. Obs-calc diagrams from refinements of $MnCl_{0.7}OH_{1.3}$ (a) and $MnCl_2$ against the first phase crystallizing from $MnCl_2 \cdot 4H_2O$. c) is the obs-calc diagram after refinement of $MnCl_2$ (in between stacking) against the diffractogram of the third phase to crystallize.

S4 Additional experiments to test the stabilizing effect of the chloride ions on solvated cations

The chloride precursors were generally found very stable under solvothermal conditions, most likely due to formation of complexes with strong interactions, both between cations and anions but also with the surrounding solvent molecules. To elaborate this point, at few additional experiments were performed. In the first, a 50:50 vol% mixture of $Cu(NO_3)_2 \cdot 3H_2O$ and $CuCl_2 \cdot 2H_2O$ (both 1 M) in water was used as precursor. Here, CuO was observed to crystallize in the approx. same reaction temperature/time region as for the pure $Cu(NO_3)_2 \cdot 3H_2O$ precursor, however with lower intensity (Figure S4-1).

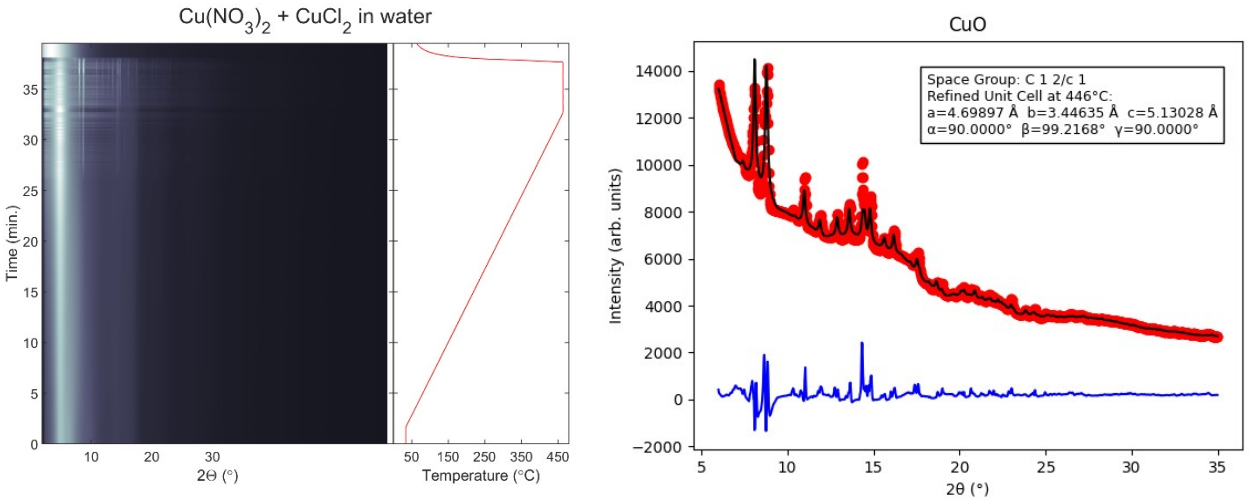

Figure S4-1. Waterfall plot of the integrated scattering data along with the temperature profile (left) and obs-calc diagram after Rietveld refinement of CuO. Please note that the detector images contained spots from single crystals, which skewed the relative intensities of Bragg reflections as well as the peak shape after integration and thereby decreased the goodness of fit.

Three additional precursors were prepared by adding approx. 0.2 ml of concentrated hydrochloric acid (37%) to 0.5 ml of the aqueous precursors of $Cu(NO_3)_2 \cdot 3H_2O$, $CuSO_4 \cdot 5H_2O$, and $Cu(ace)_2 \cdot H_2O$ to obtain approx. concentrations of 0.71 M Cu^{2+} and 4 M Cl^-. The addition of HCl forced a shift of color from blue to green as seen in Figure S4-2 (a), which indicates a shift from the octahedral complex $[Cu(OH_2)_6]^{2+}$ to the tetrahedral complex $[CuCl_4]^{2-}$. Only two of the new precursors were subjected to hydrothermal treatment due to time constraints, and crystallization was not observed from any of these was as it can be seen from the lack of Bragg peaks (present as bright vertical lines) in the waterfall plots of the diffractograms in Figure S4-2 (b) and (c).

In summary, the results confirm the precursor-stabilizing effect of chloride ions and points towards a lower limit of the chloride ion to metal ion ratio, *i.e.* that a certain amount of chloride ions is necessary to hinder crystallization under hydrothermal conditions.

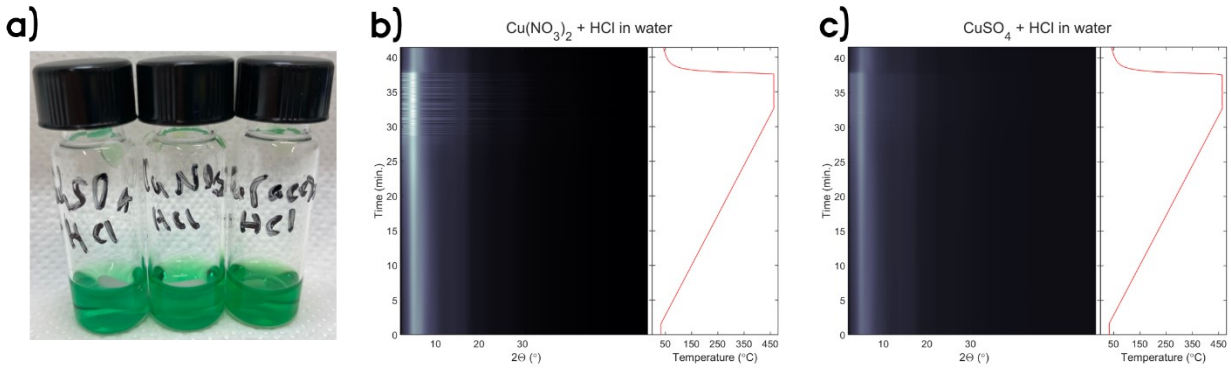

Figure S4-2. Precursors after addition of HCl (a), and waterfall plot of the integrated scattering data along with the temperature profile (b) and (c). For (a), $CuSO_4 \cdot 5H_2O$, $Cu(NO_3)_2 \cdot 3H_2O$, and $Cu(ace)_2 \cdot H_2O$ are shown left to right, respectively.

S5 Time-resolved diffractograms, heating profiles and obs-calc diagrams of refined phases

In the following, time-resolved diffractograms are presented as waterfall plots for each solvothermal *in situ* experiment along with the measured heating profile. Bragg peaks stand out as bright vertical lines. For each refined phase, obs-calc diagrams are plotted along with information on the space group and unit cell parameter at the corresponding temperature. For all obs-calc diagrams, the observed data points are red dots, the modelled diffractogram is black and the difference curve blue. Comments concerning the experiments or data processing are provided when relevant.

S5.1 $Co(acac)_2$ in ethanol

The unknown phase present prior to heating is most likely a polymorph of $Co(acac)_2$, but this could not be confirmed because of lacking database matches and weak intensity of the reflections.

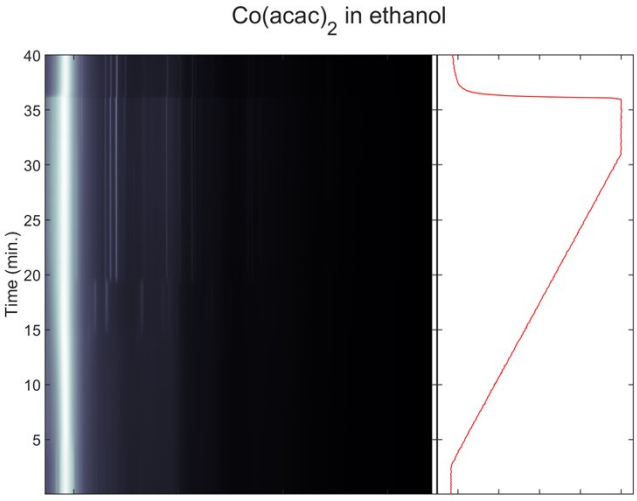

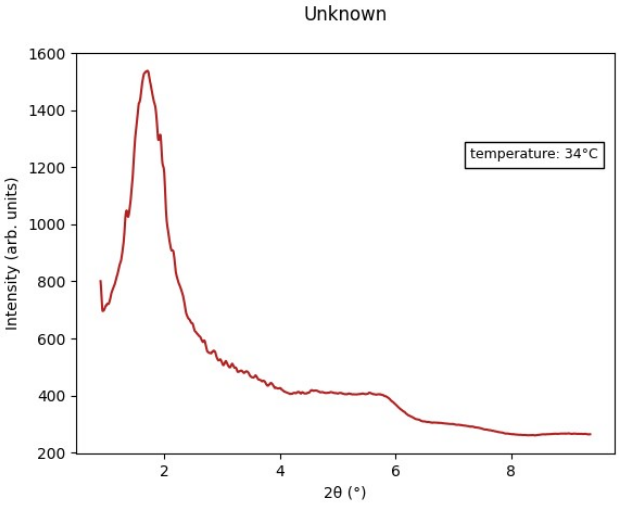

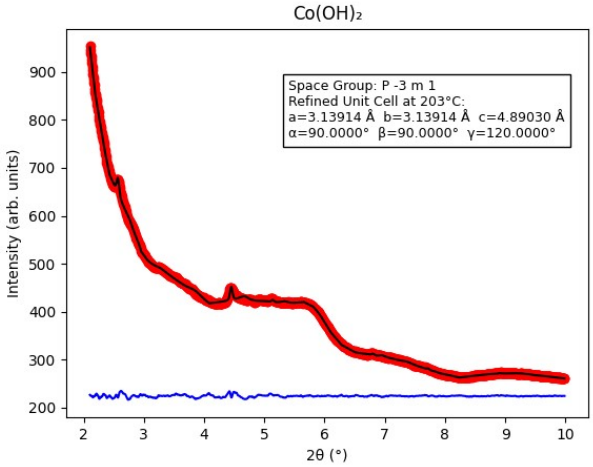

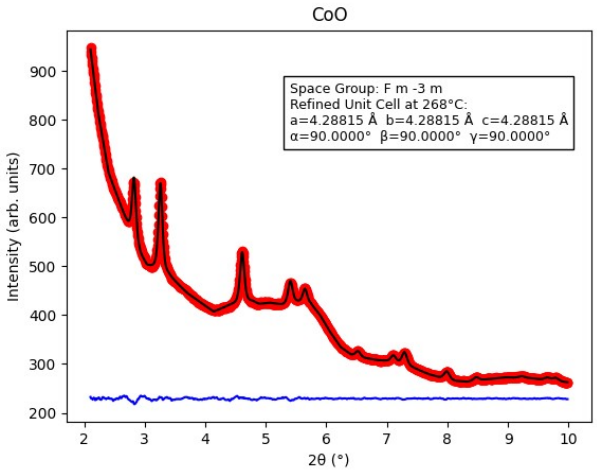

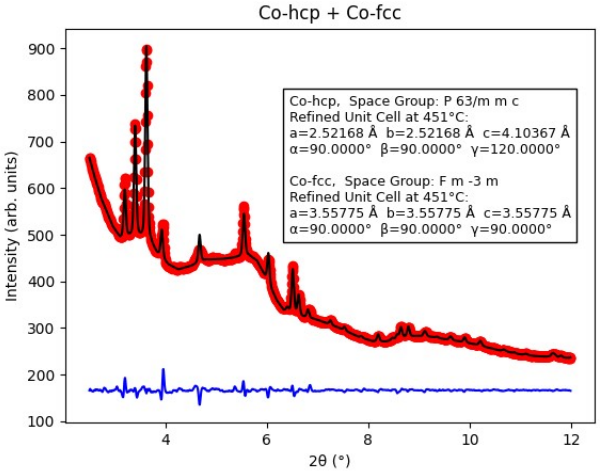

S5.2 $Co(ace)_2 \cdot 4H_2O$ in ethanol

The unknown phase present prior to heating is most likely $Co(ace)_2 \cdot xH_2O$, but this could not be confirmed because of lacking database matches and weak intensity of the reflections.

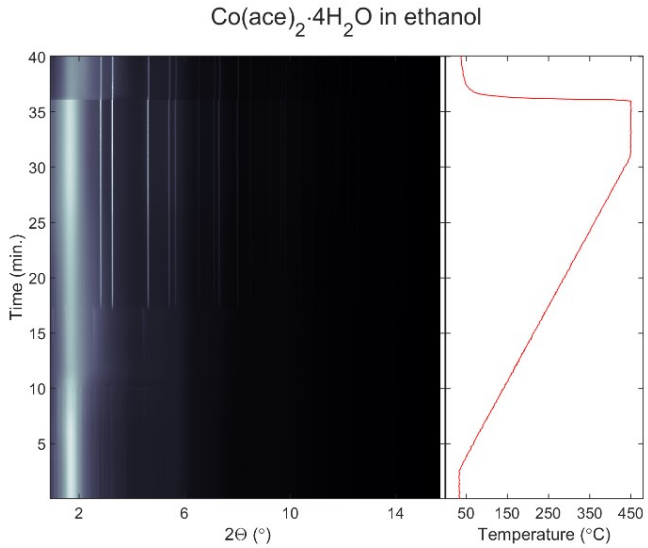

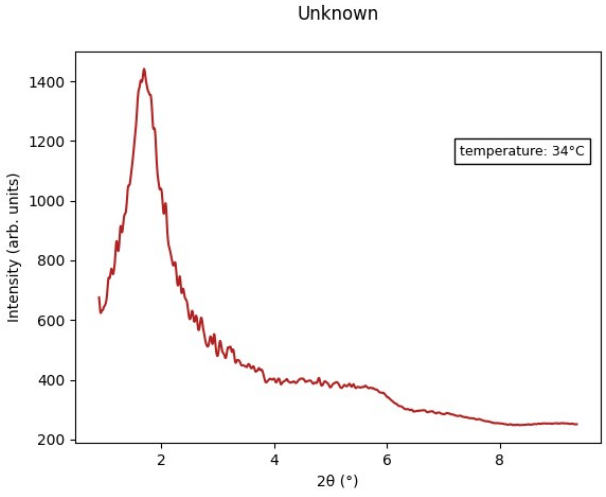

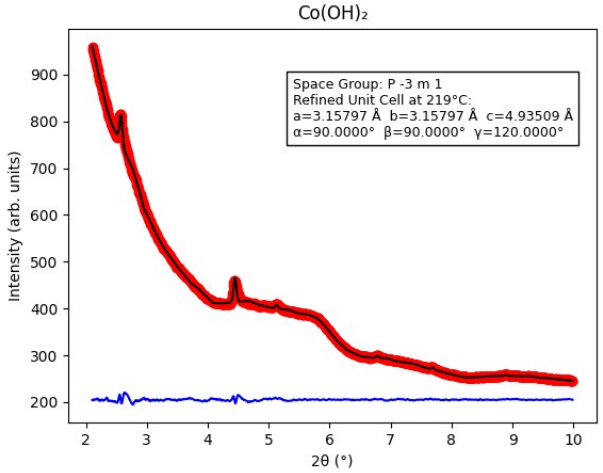

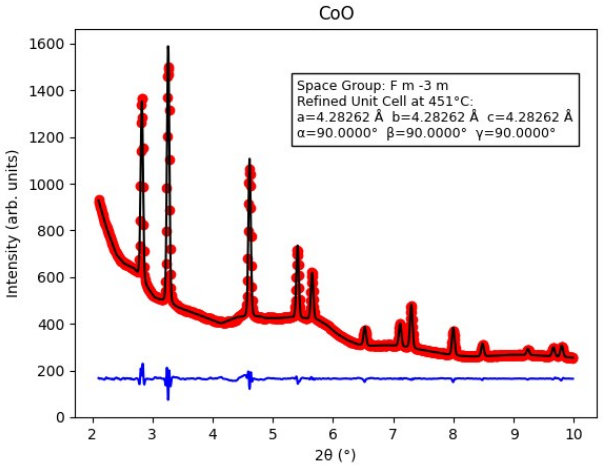

S5.3 $CoCl_2 \cdot 6H_2O$ in ethanol

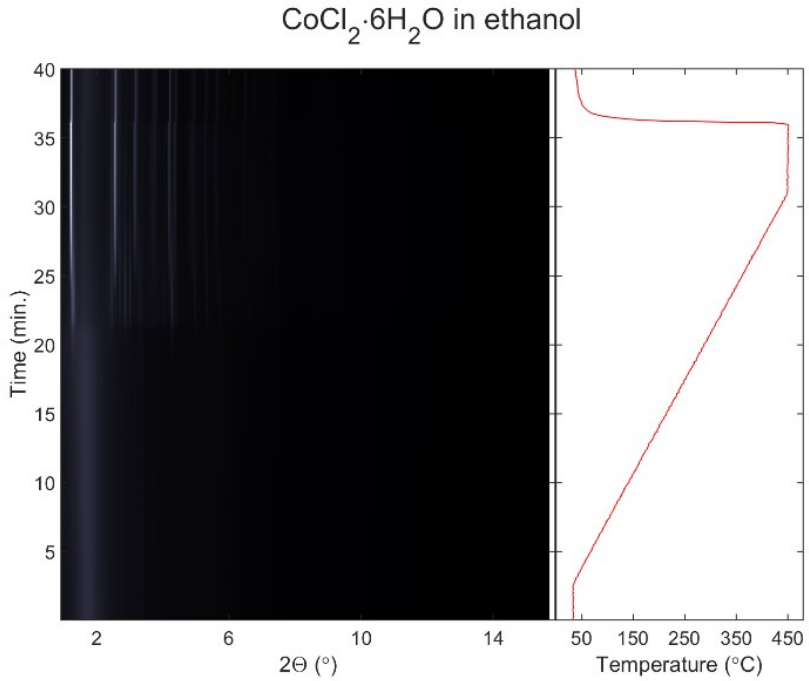
$CoCl_2 \cdot 6H_2O$ in ethanol
Time (min.)
2Θ (°)
Temperature (°C)

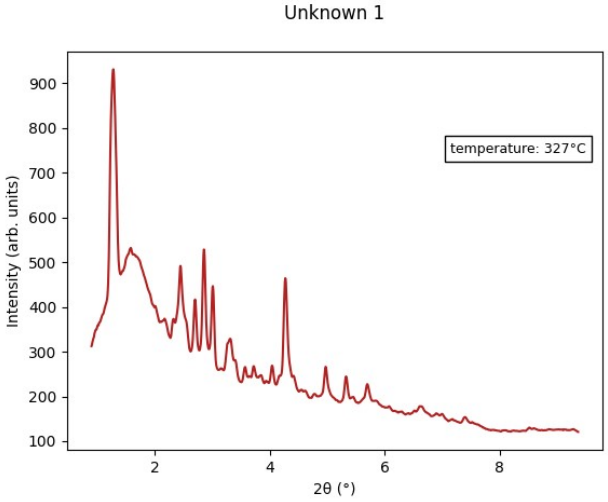
Unknown 1
temperature: 327°C
Intensity (arb. units)
2θ (°)

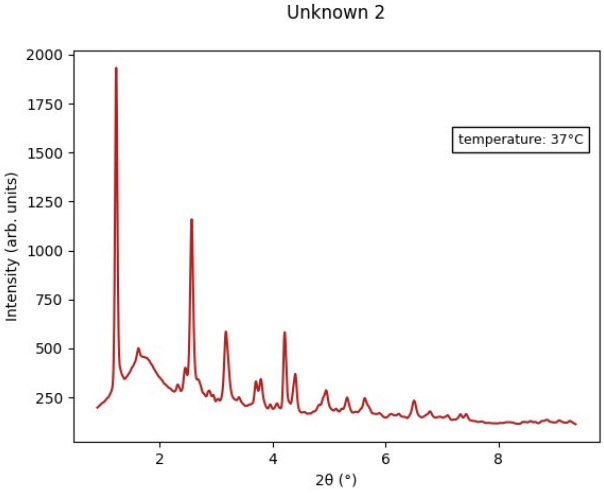
Unknown 2
temperature: 37°C
Intensity (arb. units)
2θ (°)

S5.4 CoI_2 in ethanol

Intense peaks from single crystals caused unreliable relative intensities between reflections and between subsequent diffractograms.

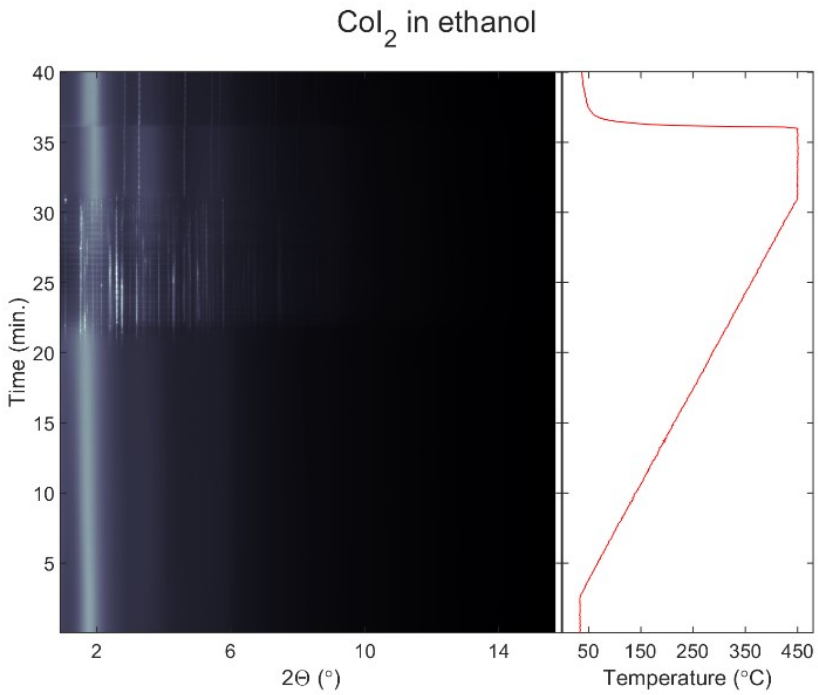

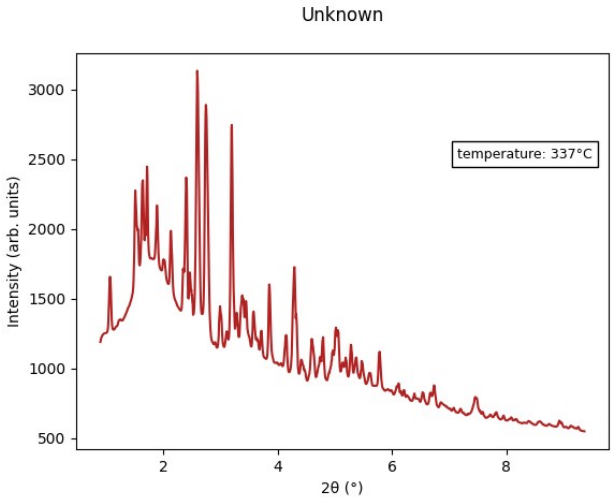

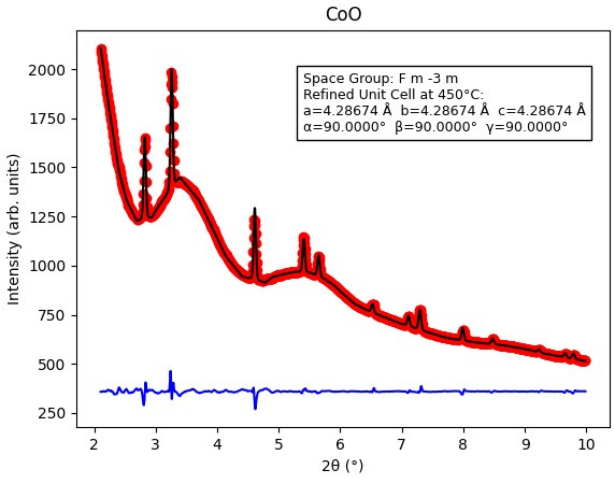

S5.5 $Co(NO_3)_2 \cdot 6H_2O$ in ethanol

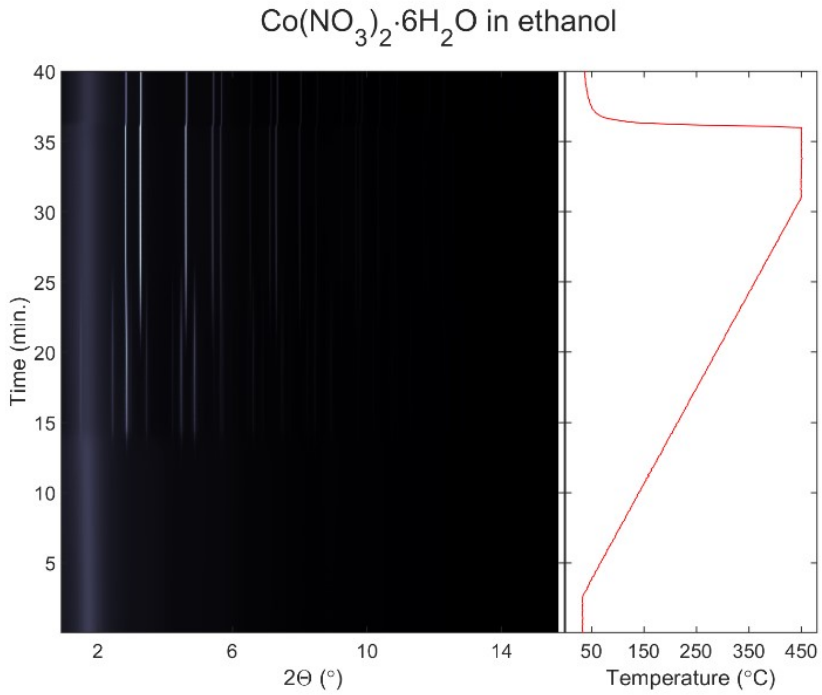

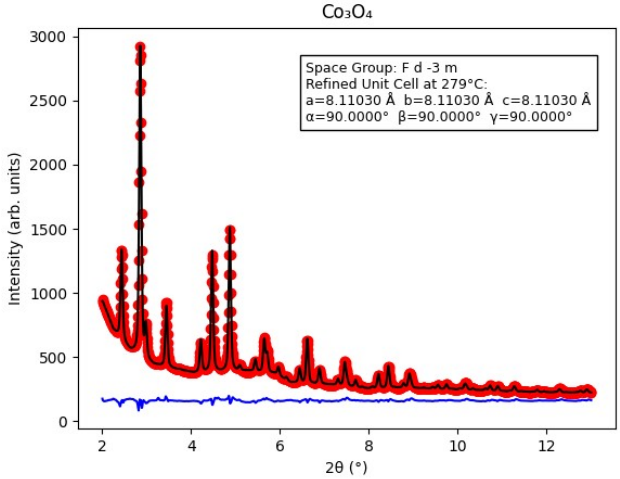

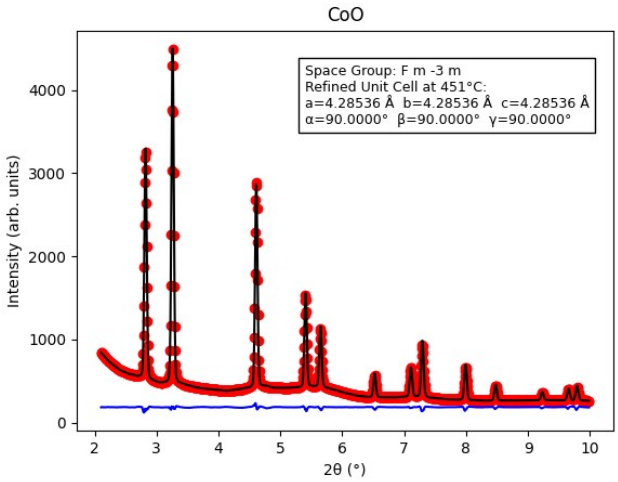

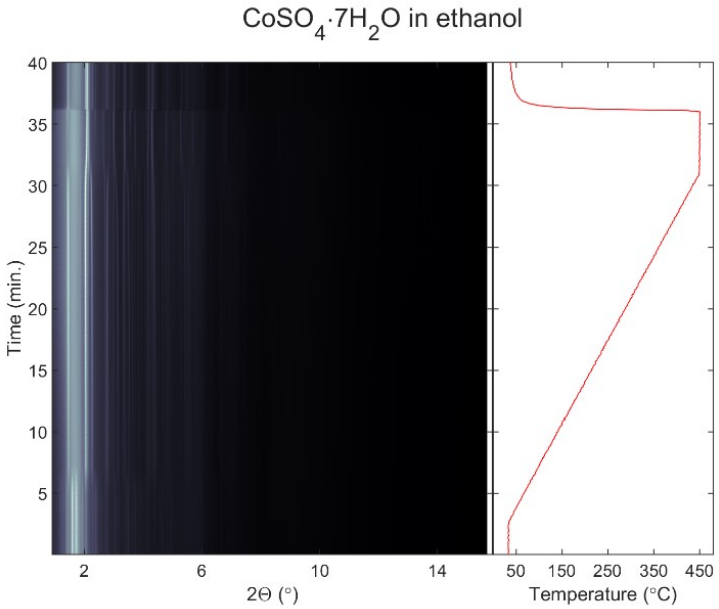

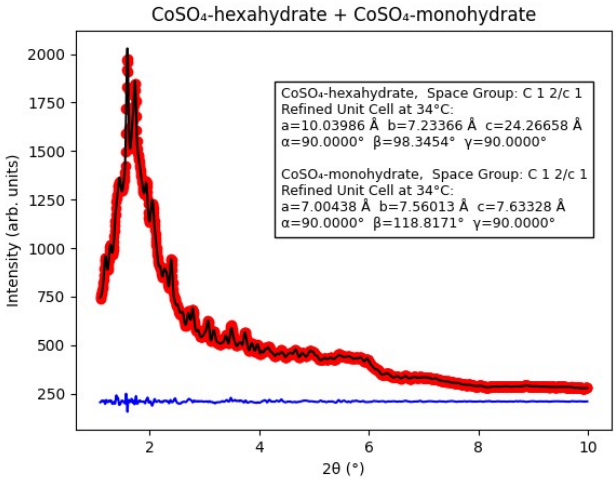

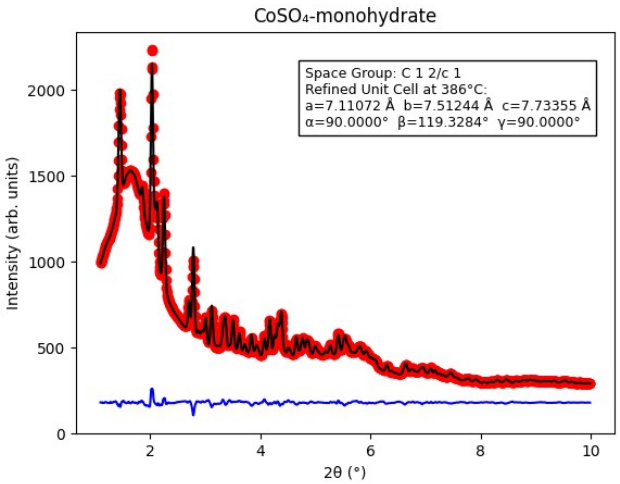

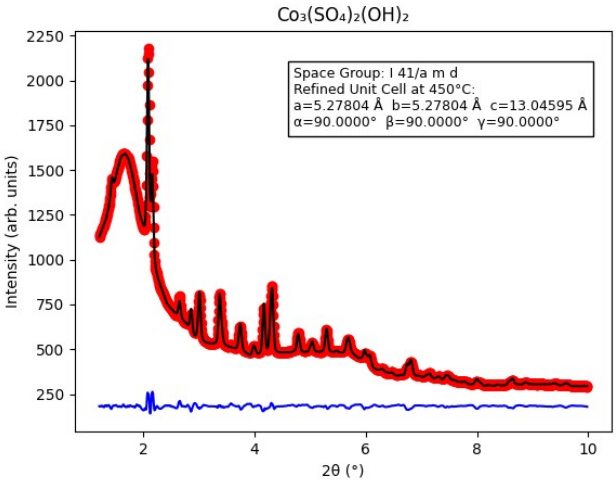

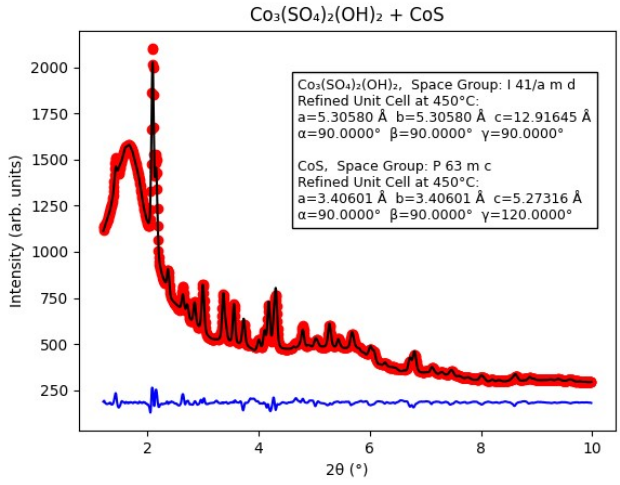

S5.6 $CoSO_4 \cdot 7H_2O$ in ethanol

S5.7 $Cu(acac)_2$ in ethanol

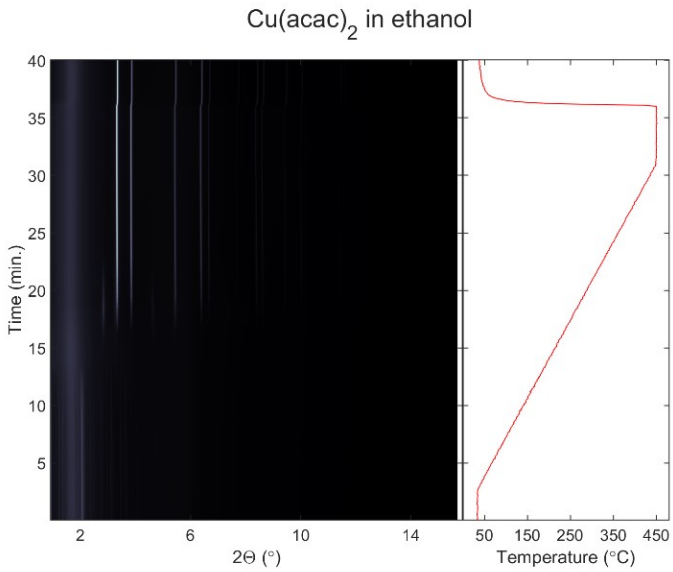
Cu(acac)2 in ethanol
Time (min.)
2Θ (°)
Temperature (°C)

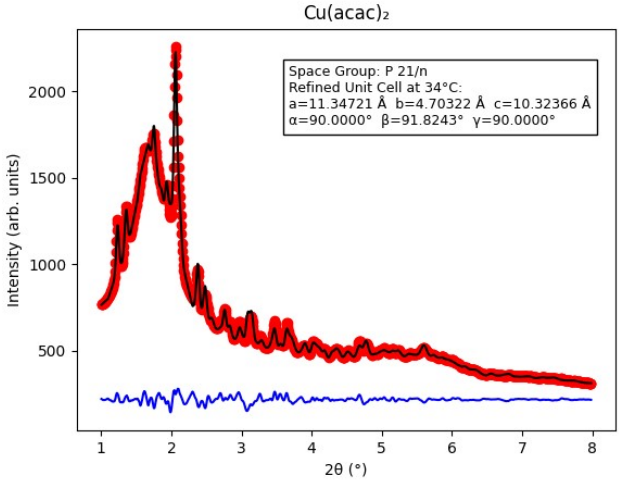
Cu(acac)₂
Space Group: P 21/n
Refined Unit Cell at 34°C:
a=11.34721 Å b=4.70322 Å c=10.32366 Å
α=90.0000° β=91.8243° γ=90.0000°
Intensity (arb. units)
2θ (°)

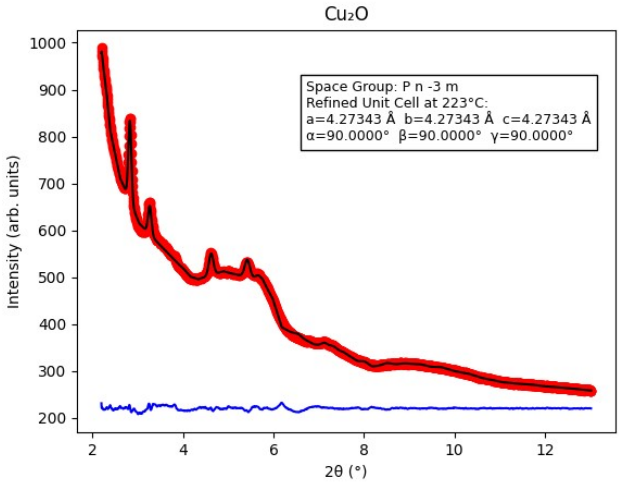
Cu₂O
Space Group: P n -3 m
Refined Unit Cell at 223°C:
a=4.27343 Å b=4.27343 Å c=4.27343 Å
α=90.0000° β=90.0000° γ=90.0000°
Intensity (arb. units)
2θ (°)

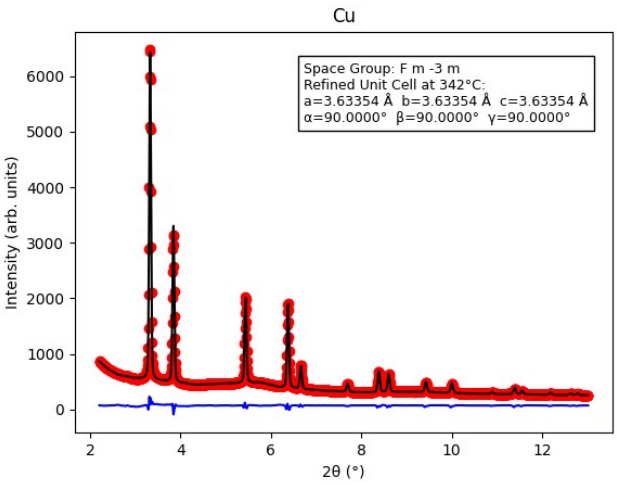
Cu
Space Group: F m -3 m
Refined Unit Cell at 342°C:
a=3.63354 Å b=3.63354 Å c=3.63354 Å
α=90.0000° β=90.0000° γ=90.0000°
Intensity (arb. units)
2θ (°)

S5.8 $Cu(ace)_2 \cdot H_2O$ in ethanol

The initial unknown phases (1 & 2) are likely polymorphs of $Cu(ace)_2 \cdot xH_2O$ and $Cu(ace)_2$, but this could not be confirmed because of lacking database matches and weak intensity of the reflections.

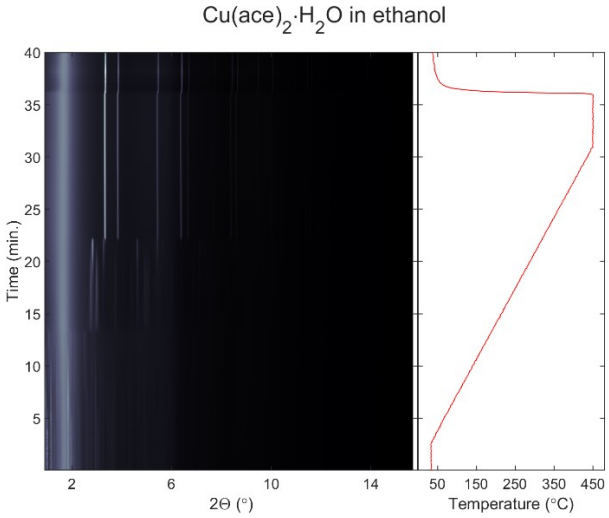

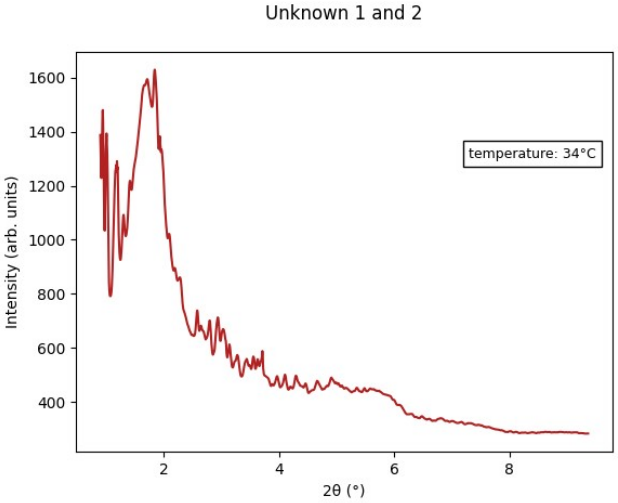

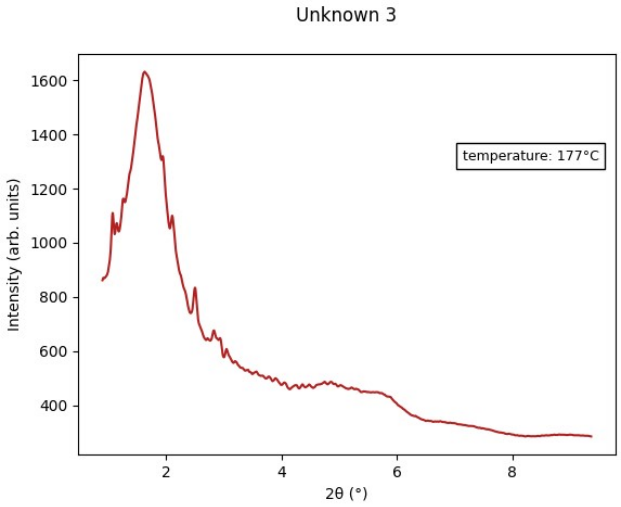

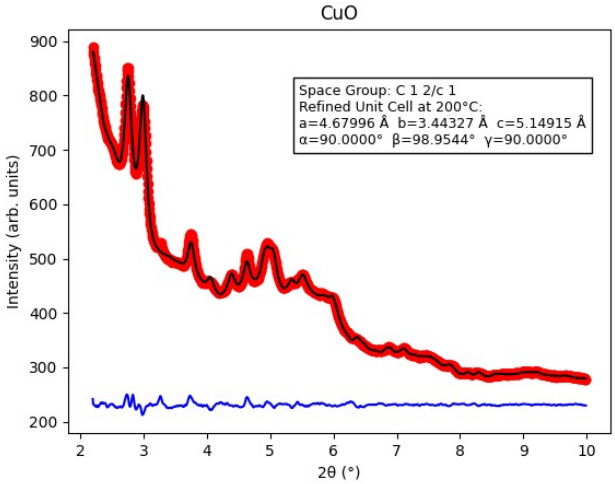

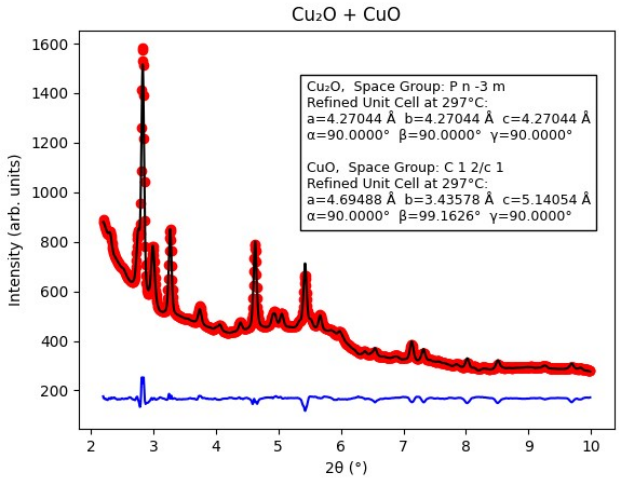

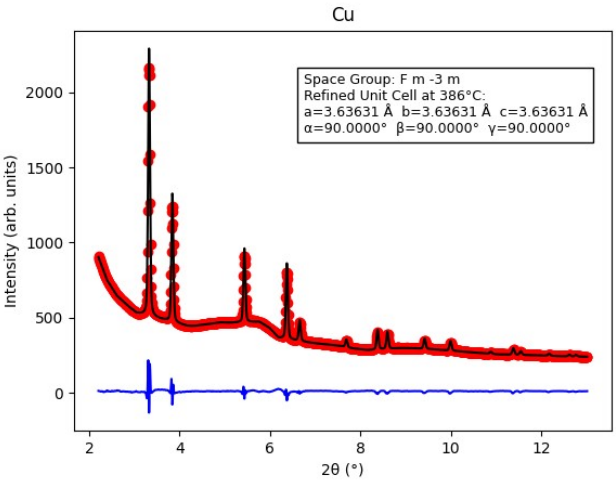

S5.9 $CuCl_2 \cdot 2H_2O$ in ethanol

Intense peaks from single crystals caused unreliable relative intensities between reflections and between subsequent diffractograms.

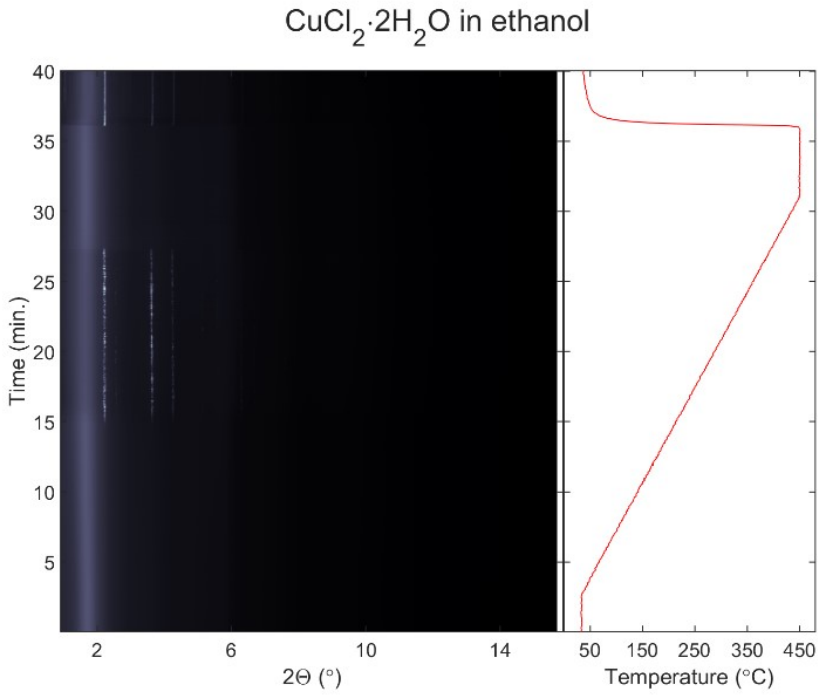

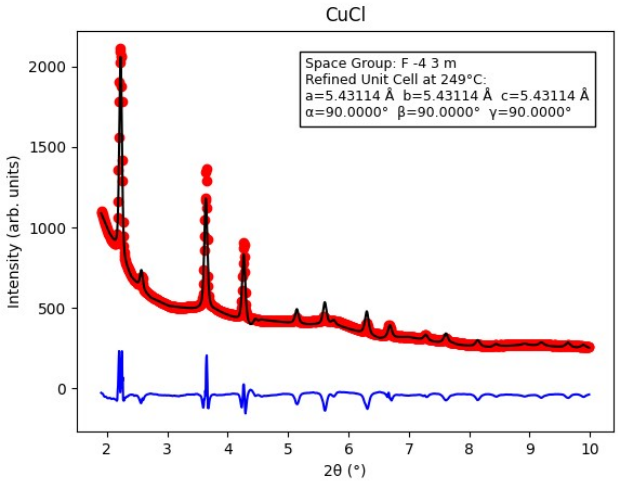

S5.10 CuI in ethanol

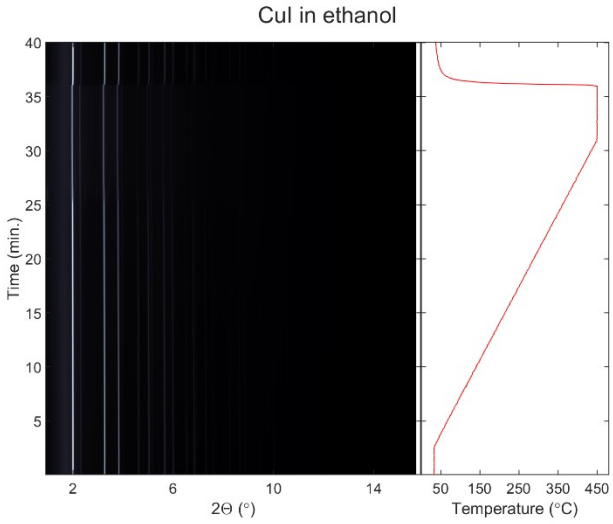

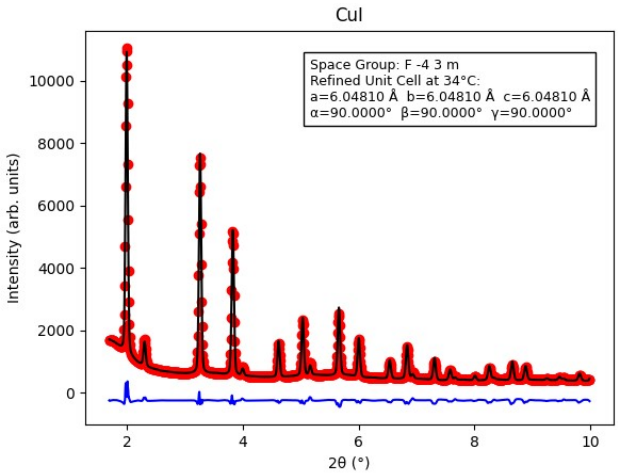

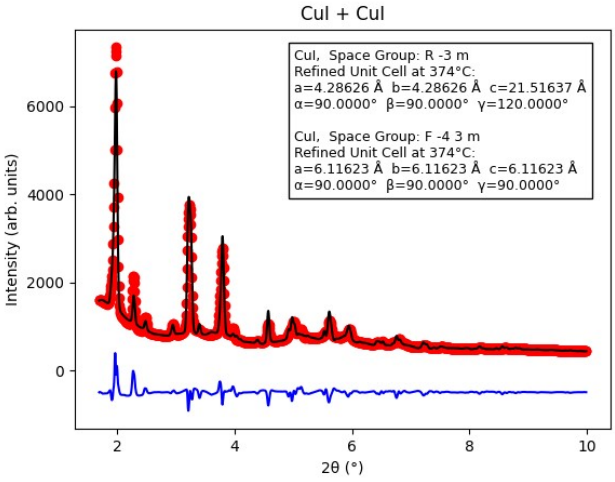

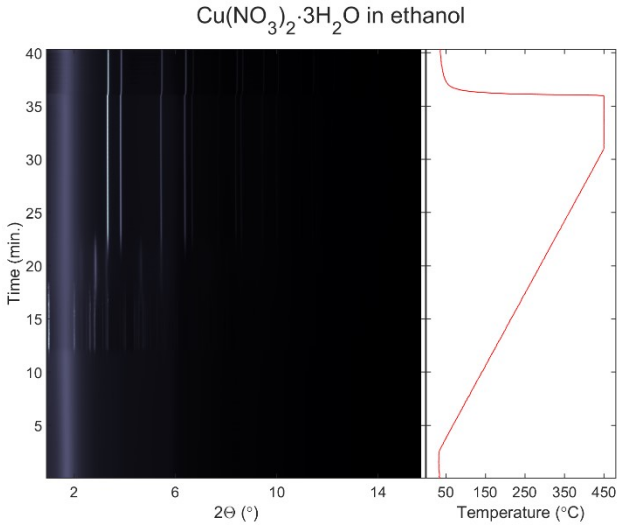

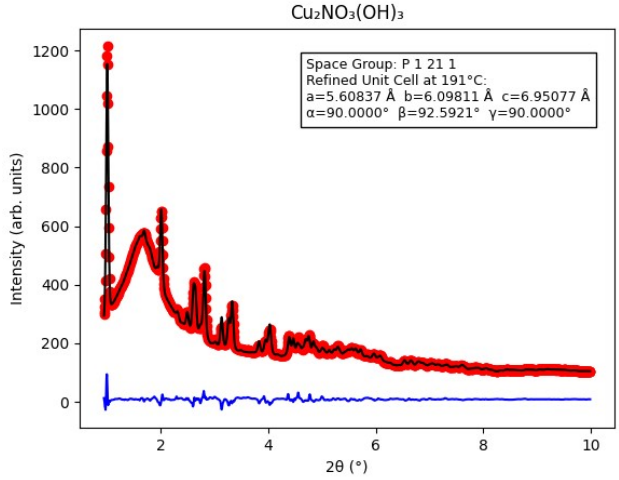

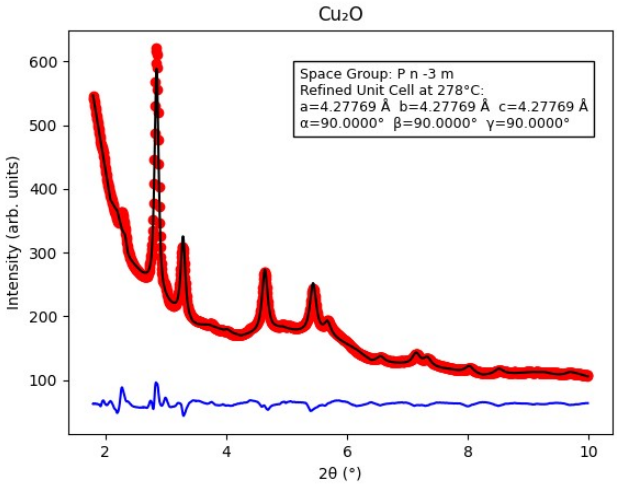

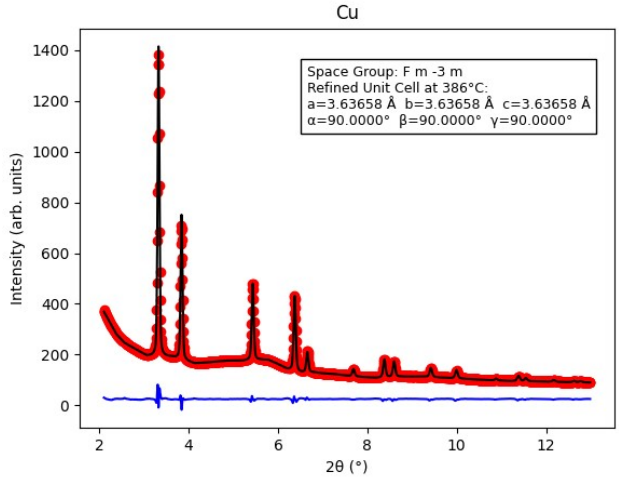

S5.11 $Cu(NO_3)_2{\cdot}3H_2O$ in ethanol

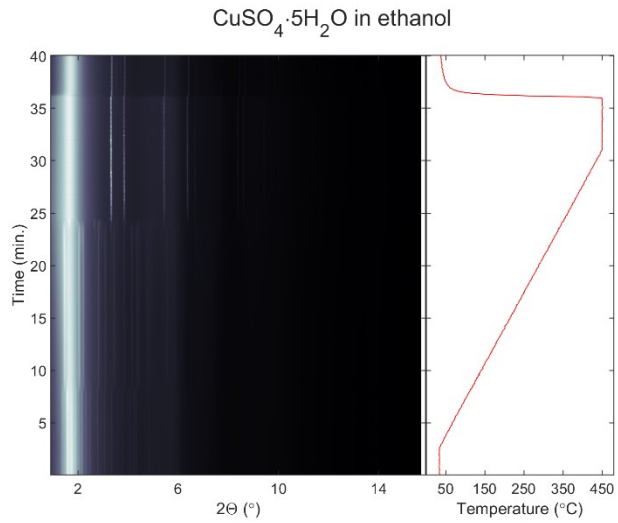

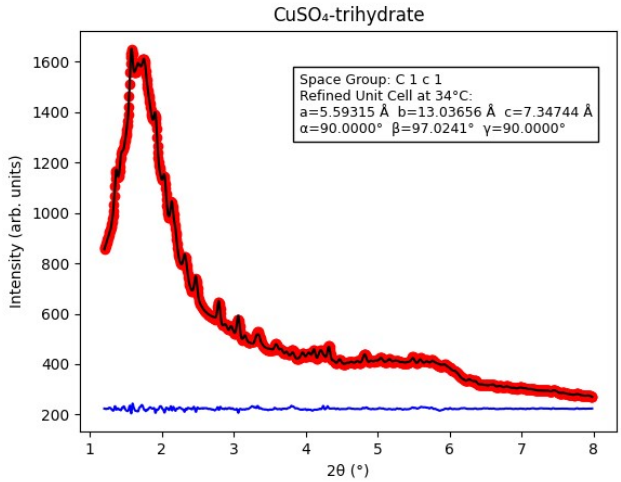

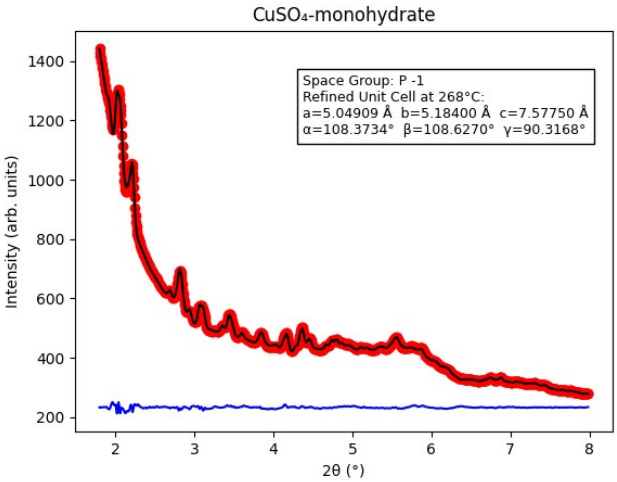

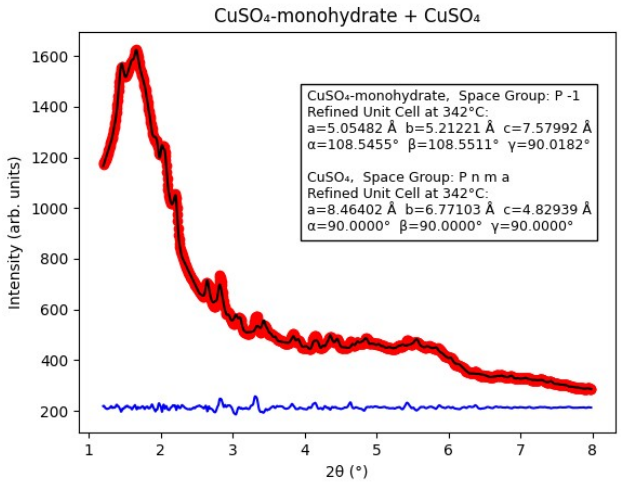

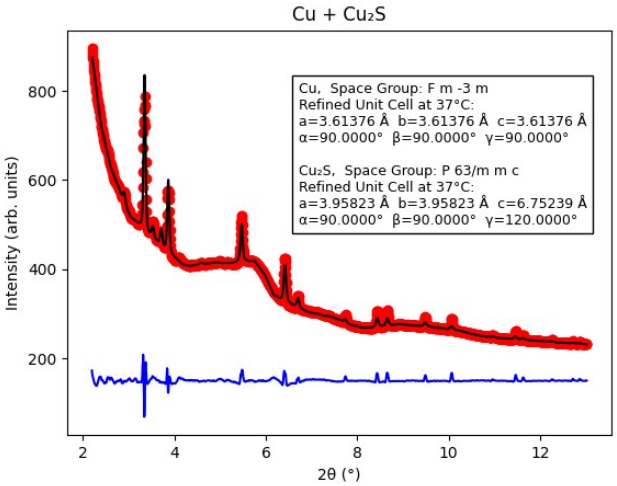

S5.12 $CuSO_4 \cdot 5H_2O$ in ethanol

S5.13 $Mn(acac)_2$ in ethanol

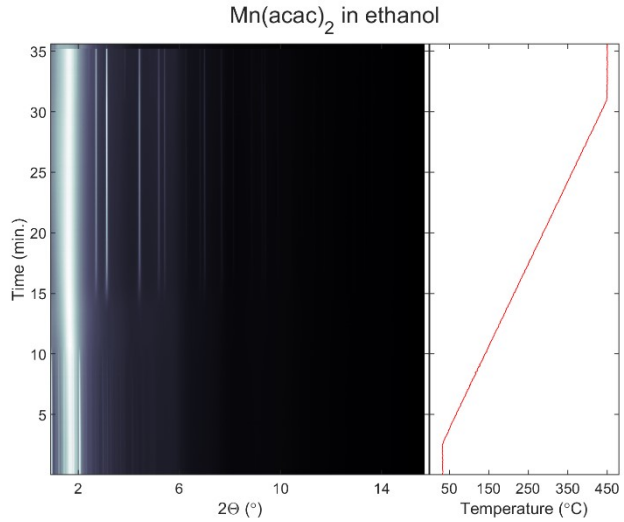

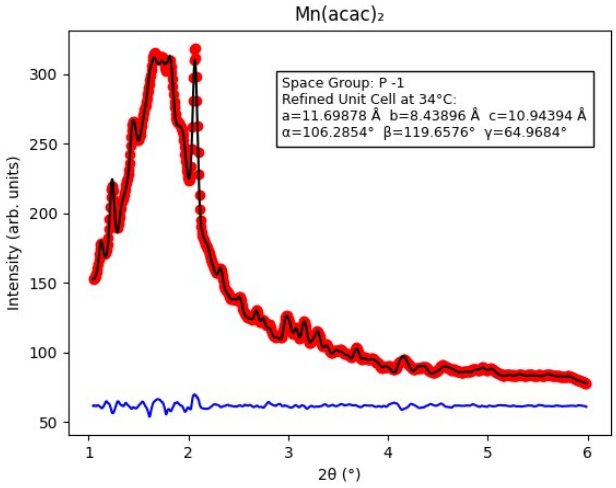

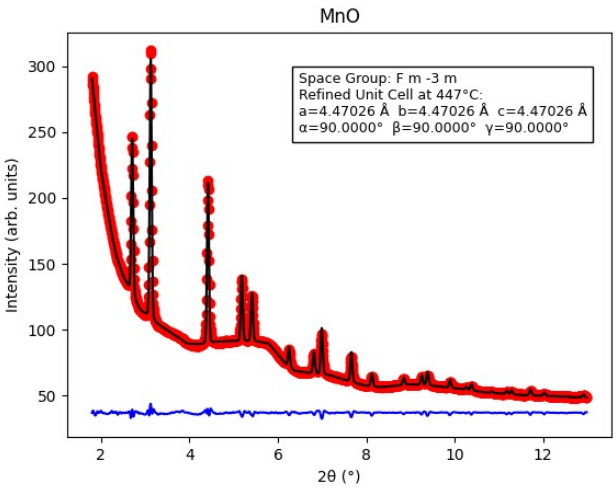

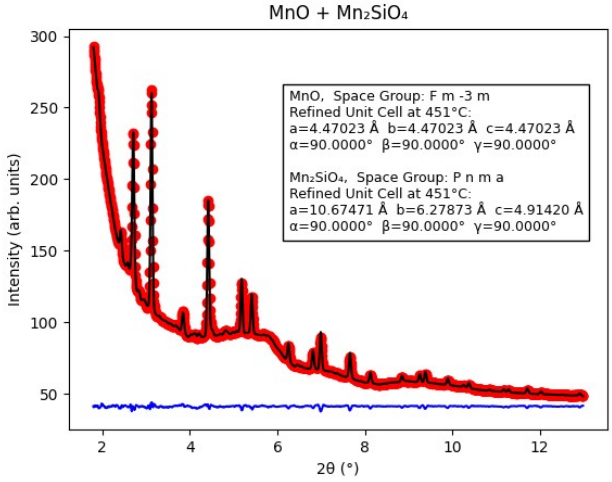

S5.14 $Mn(ace)_2 \cdot 4H_2O$ in ethanol

The initial unknown phases (1 & 2) are likely $Mn(ace)_2 \cdot xH_2O$ and $Mn(ace)_2$, but this could not be confirmed because of lacking database matches.

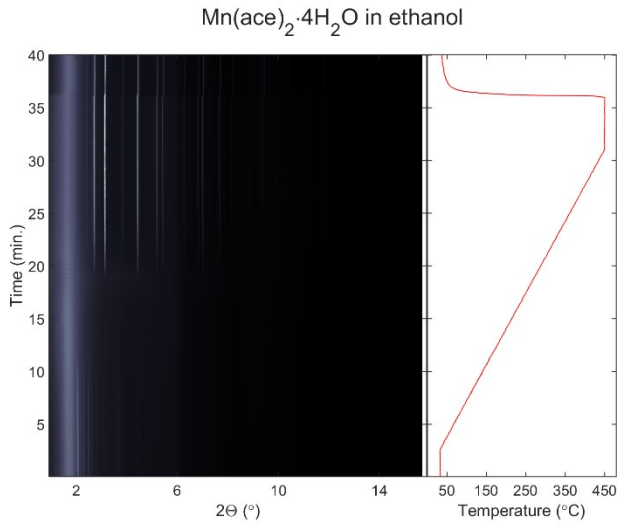

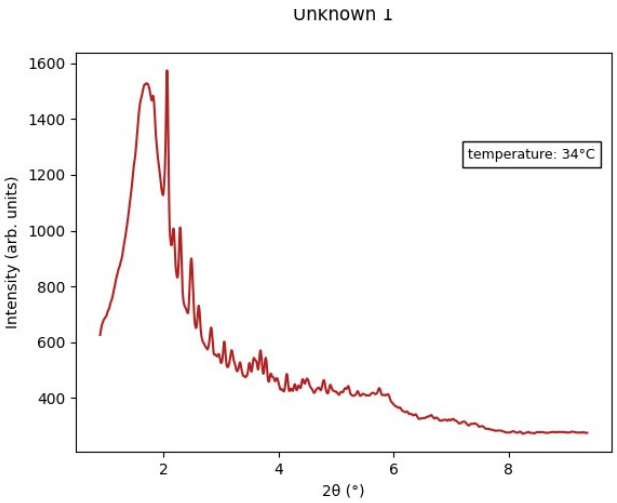

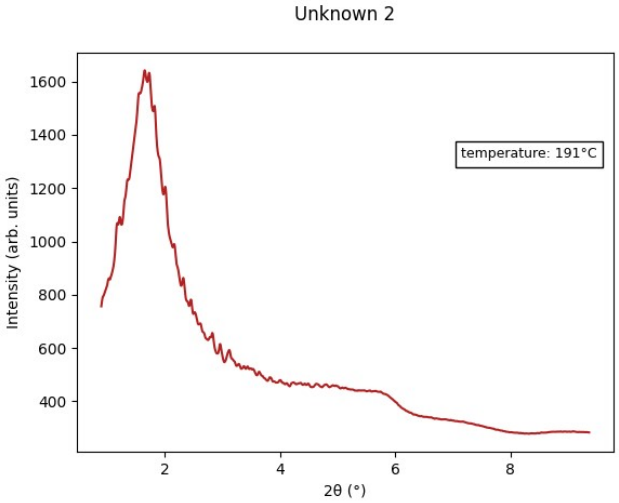

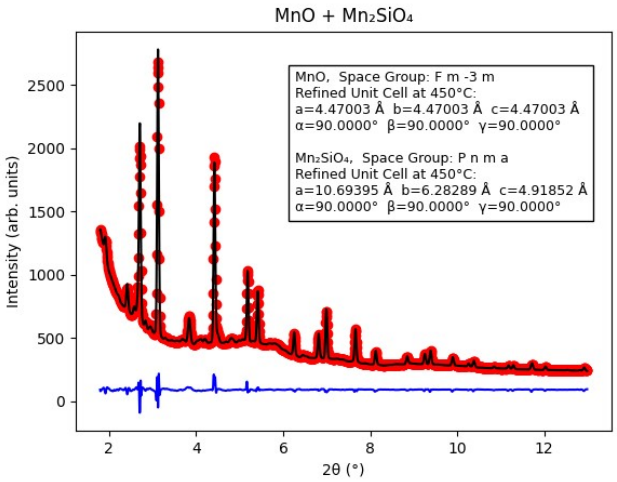

S5.15 $MnCl_2 \cdot 4H_2O$ in ethanol

Please refer to S3 for a detailed discussion of this experiment.

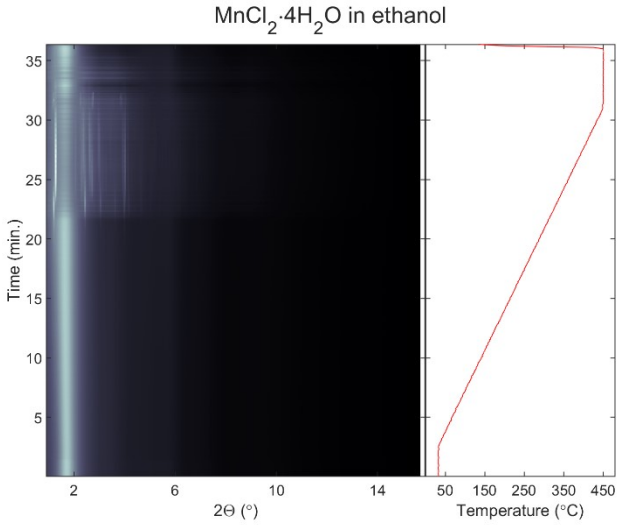

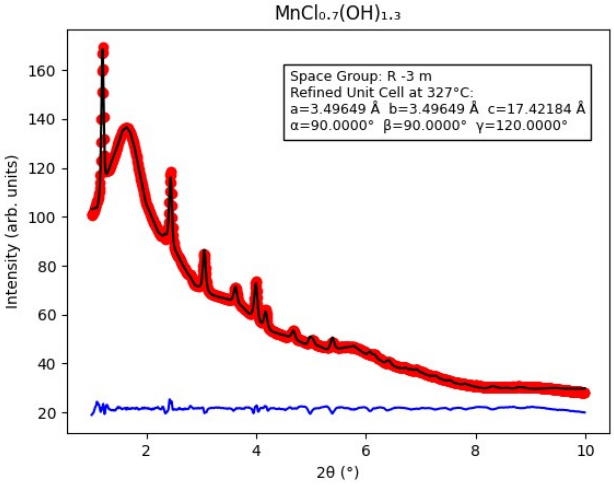

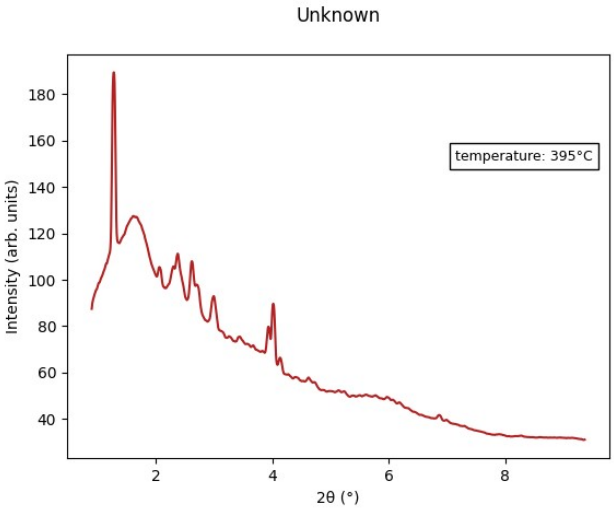

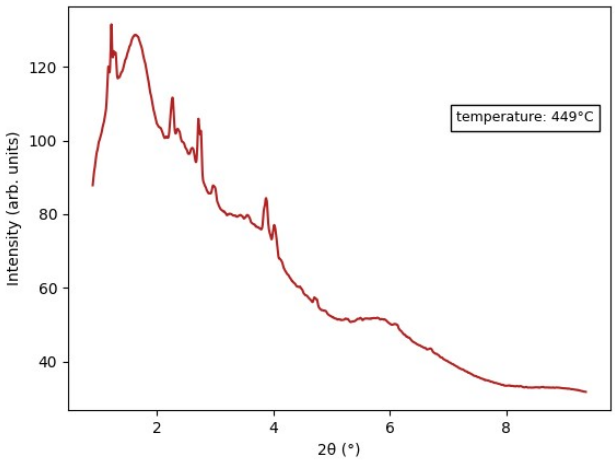

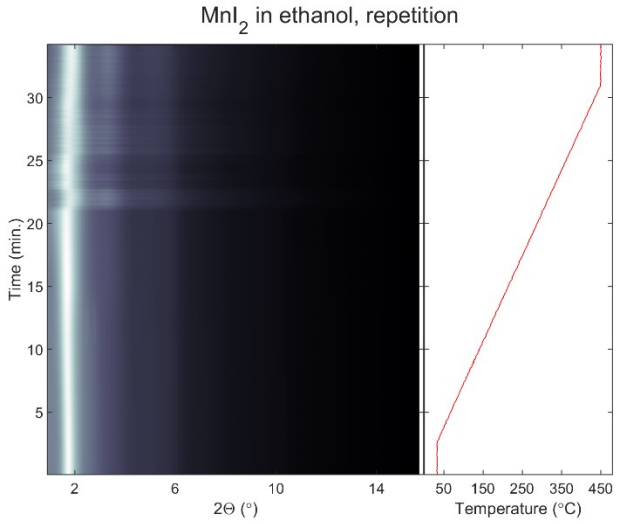

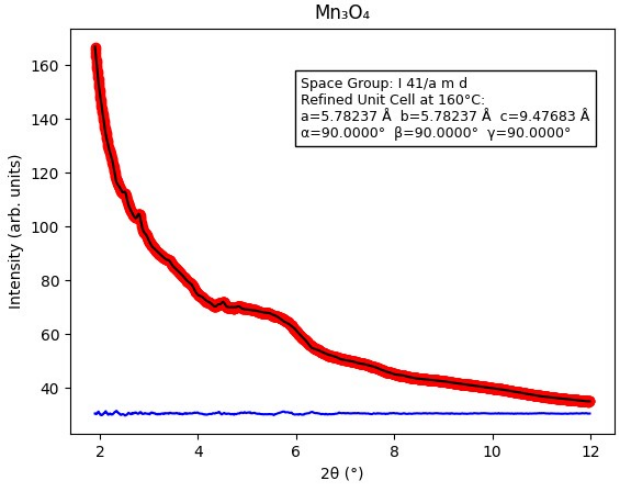

S5.16 MnI_2 in ethanol

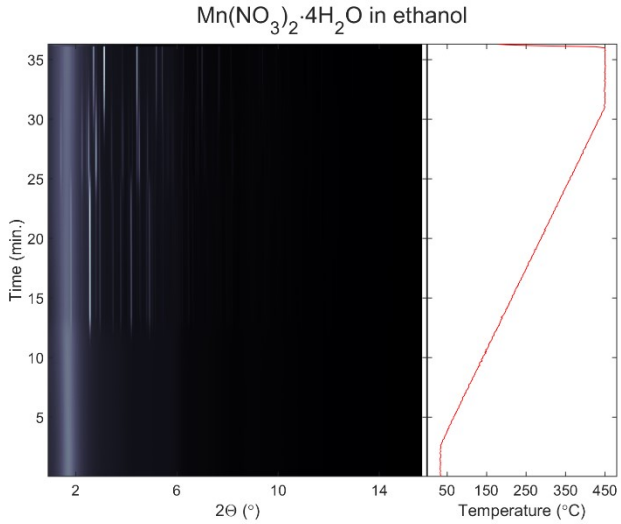

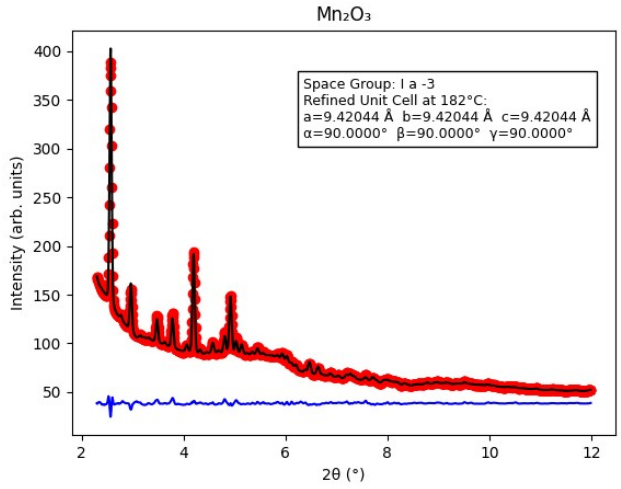

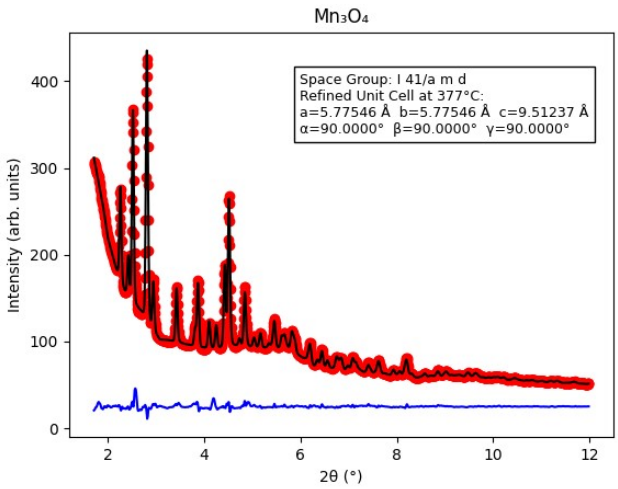

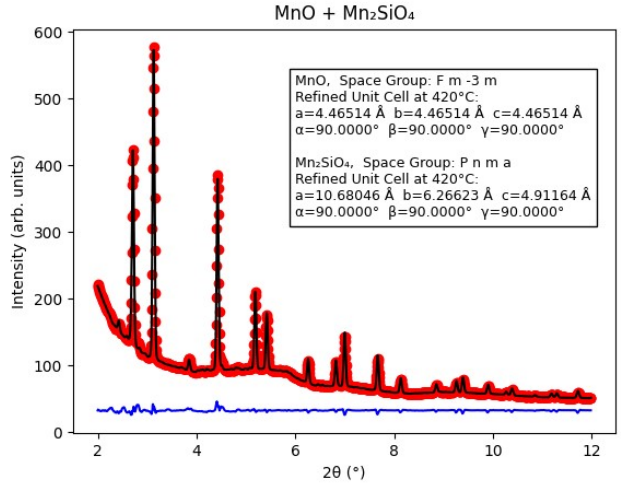

S5.17 $Mn(NO_3)_2{\cdot}4H_2O$ in ethanol

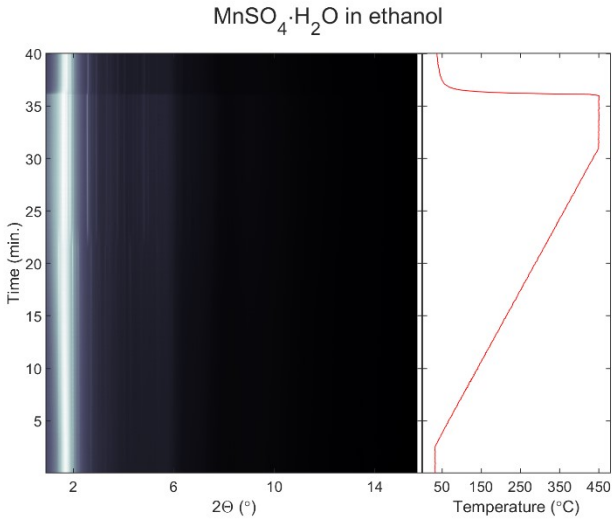

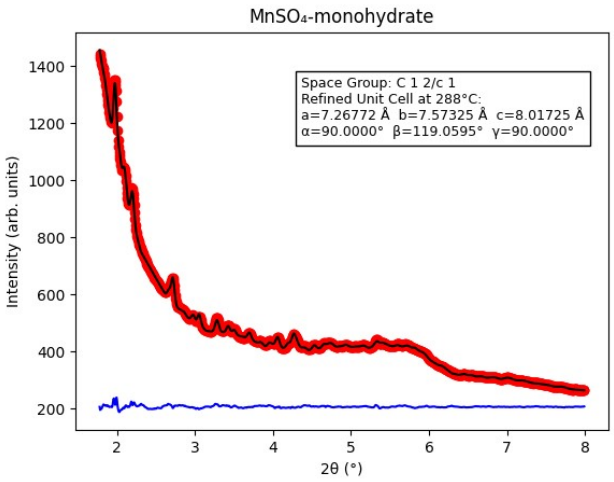

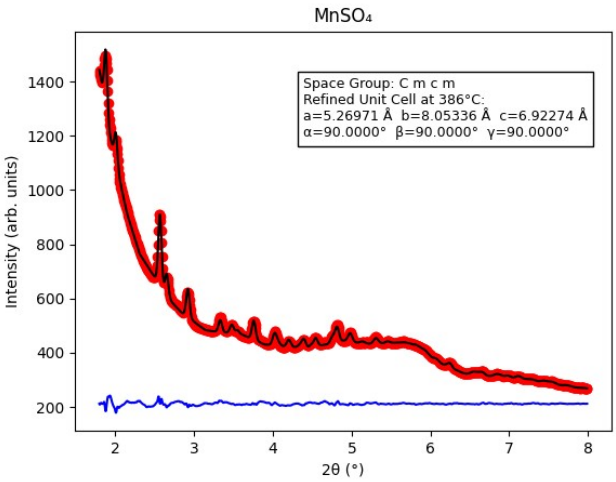

S5.18 $MnSO_4 \cdot H_2O$ in ethanol

S5.19 $Co(acac)_2$ in water

$Co(acac)_2$-dihydrate is isostructural to the manganese counterpart.

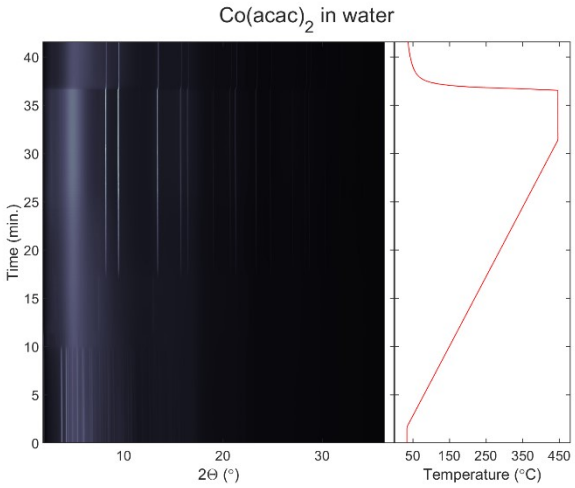
Co(acac)2 in water
Time (min.)
2Θ (°)
Temperature (°C)

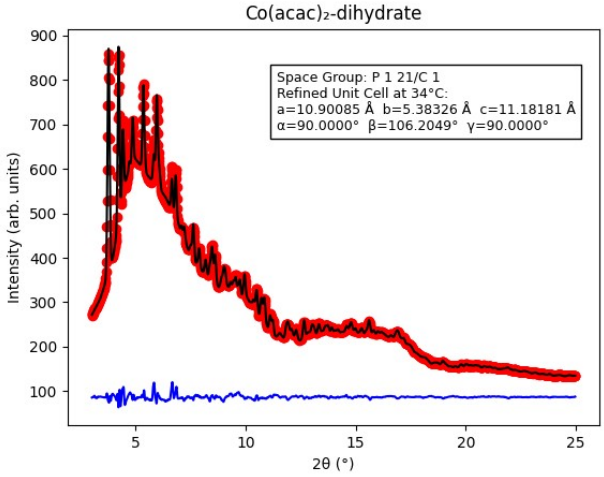
Co(acac)₂-dihydrate
Space Group: P 1 21/C 1
Refined Unit Cell at 34°C:
a=10.90085 Å b=5.38326 Å c=11.18181 Å
α=90.0000° β=106.2049° γ=90.0000°
Intensity (arb. units)
2θ (°)

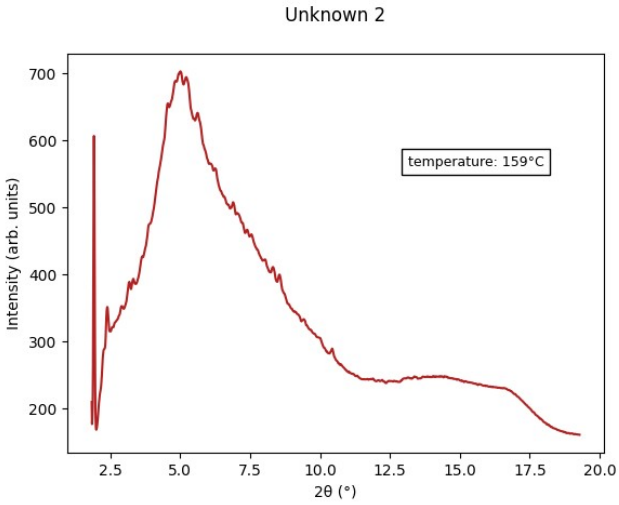
Unknown 2
temperature: 159°C
Intensity (arb. units)
2θ (°)

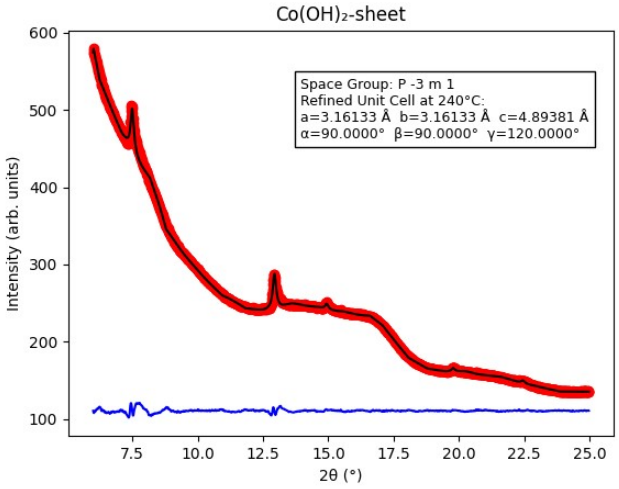
Co(OH)₂-sheet
Space Group: P -3 m 1
Refined Unit Cell at 240°C:
a=3.16133 Å b=3.16133 Å c=4.89381 Å
α=90.0000° β=90.0000° γ=120.0000°
Intensity (arb. units)
2θ (°)

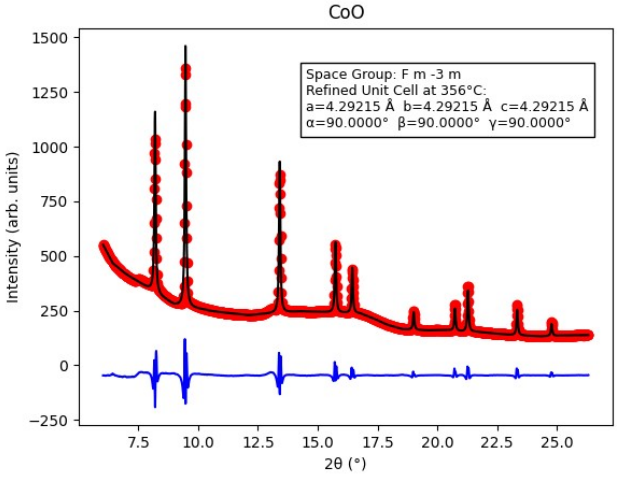
CoO
Space Group: F m -3 m
Refined Unit Cell at 356°C:
a=4.29215 Å b=4.29215 Å c=4.29215 Å
α=90.0000° β=90.0000° γ=90.0000°
Intensity (arb. units)
2θ (°)

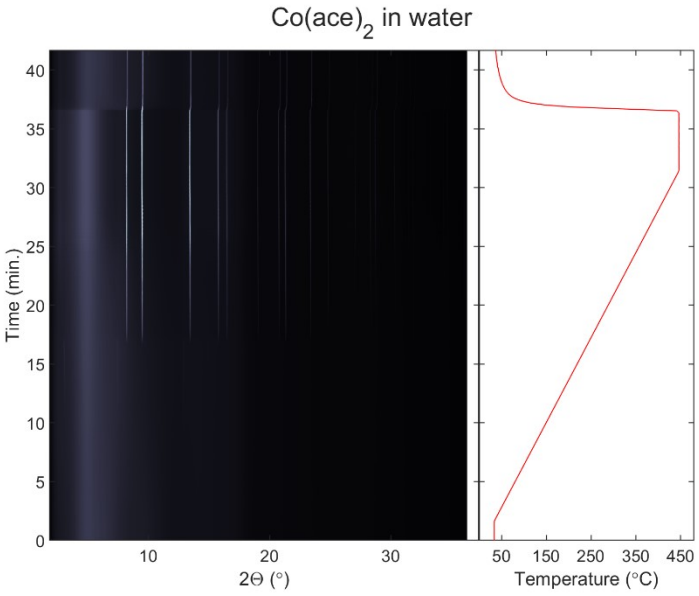

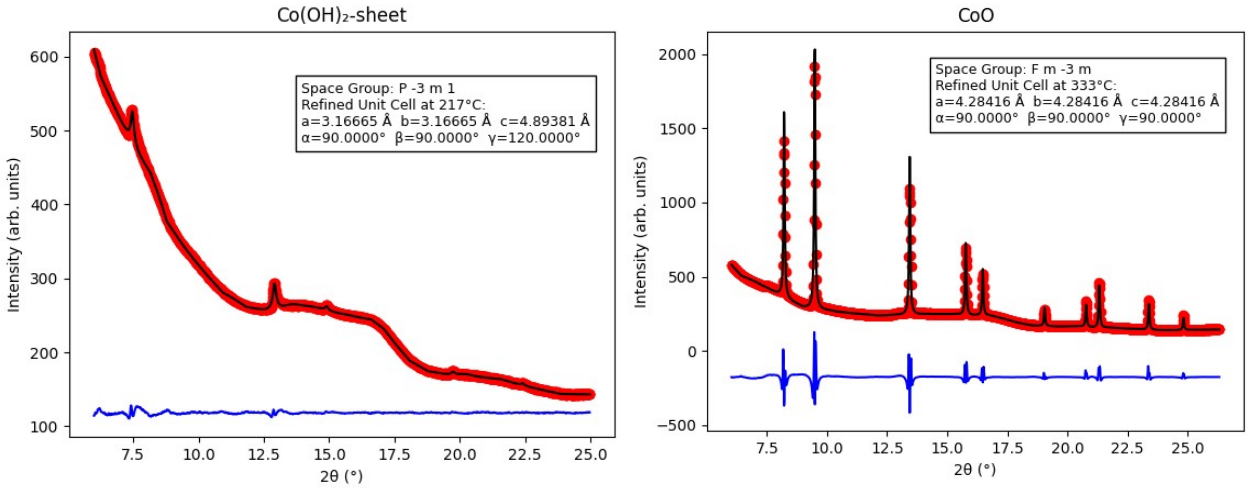

S5.20 $Co(ace)_2 \cdot 4H_2O$ in water

S5.21 $CoCl_2 \cdot H_2O$ in water

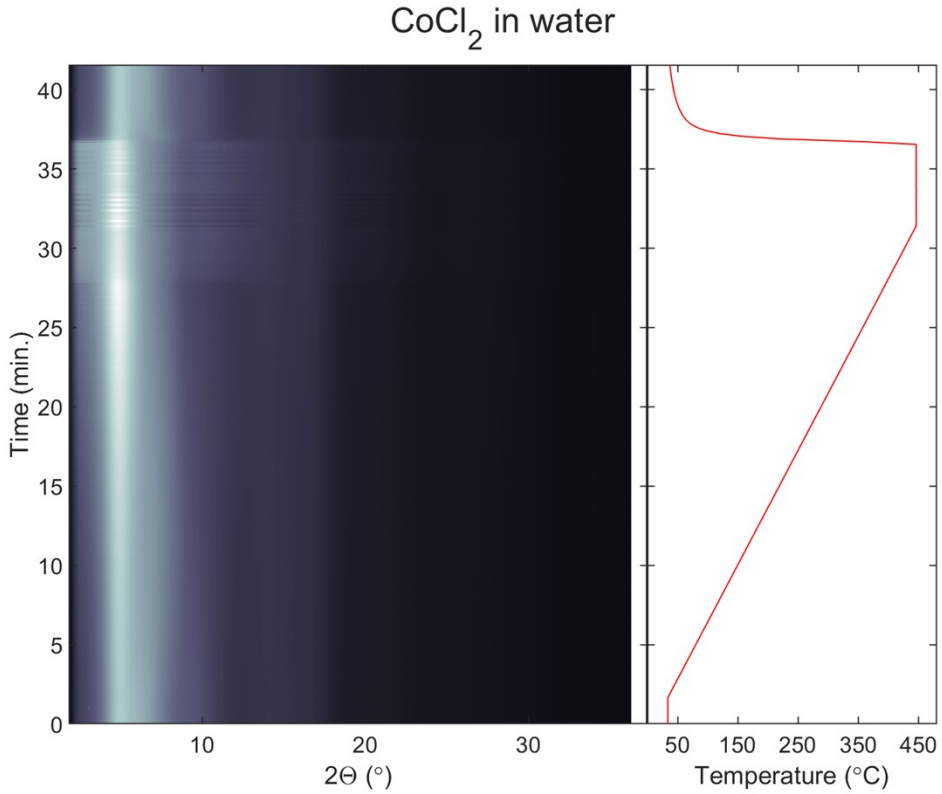

S5.22 CoI_2 in water

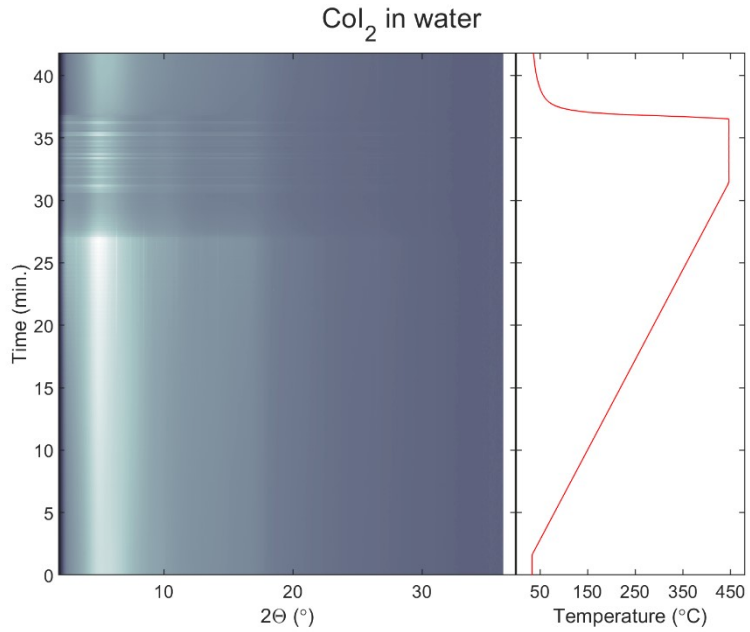

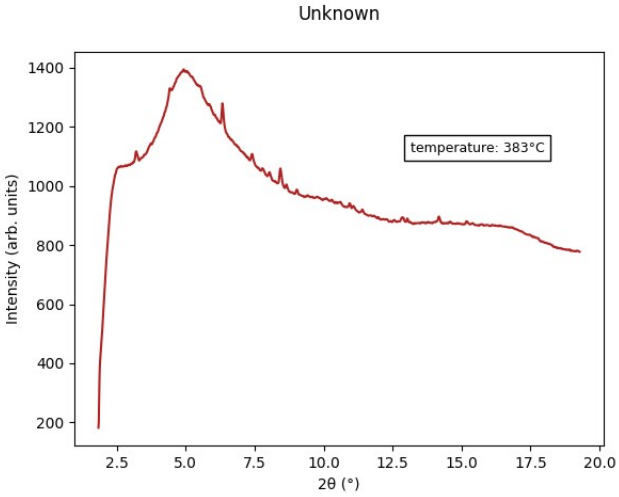

S5.23 $Co(NO_3)_2 \cdot 6H_2O$ in water

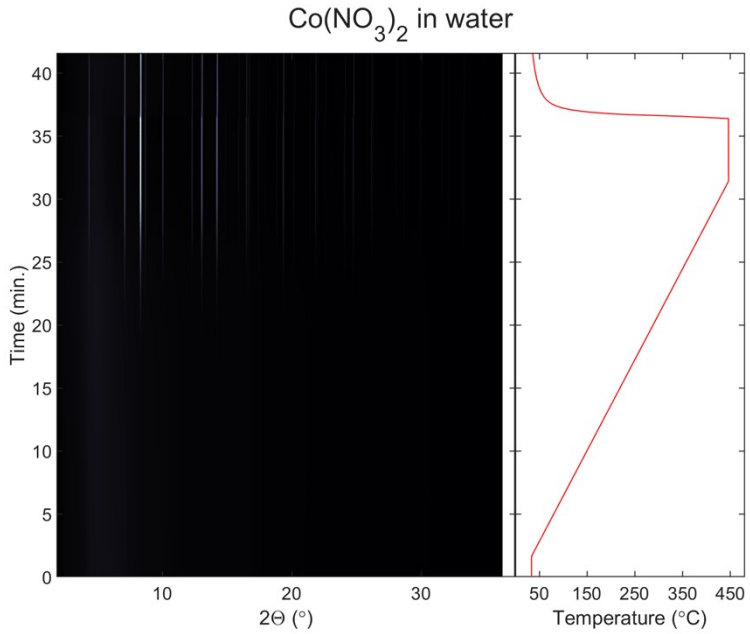

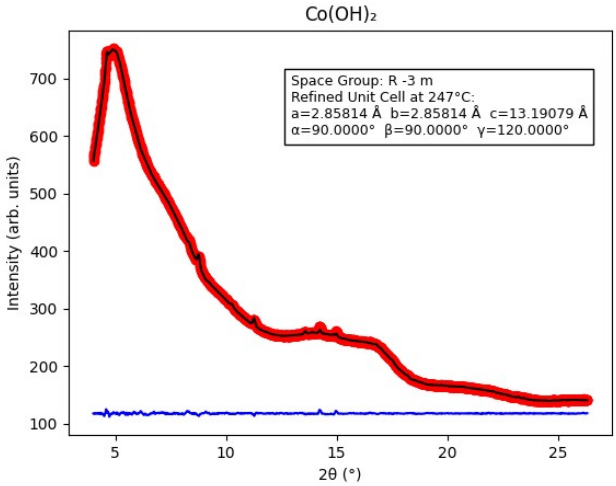

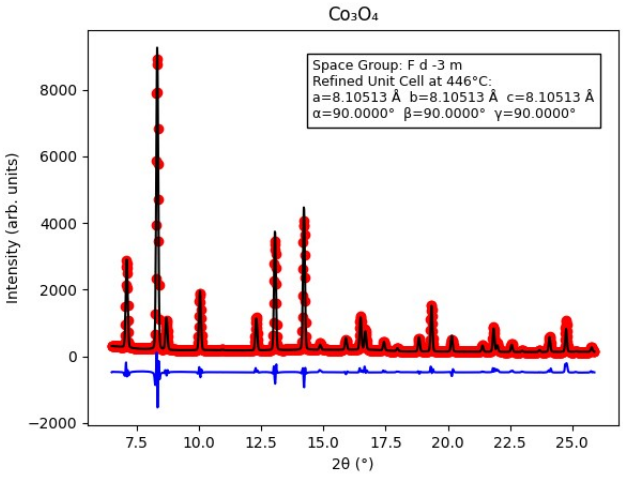

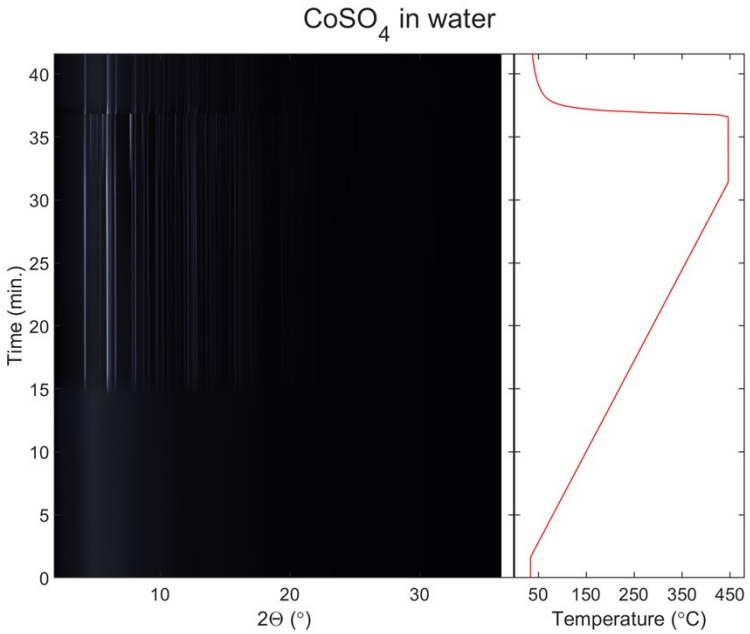

S5.24 $CoSO_4 \cdot 7H_2O$ in water

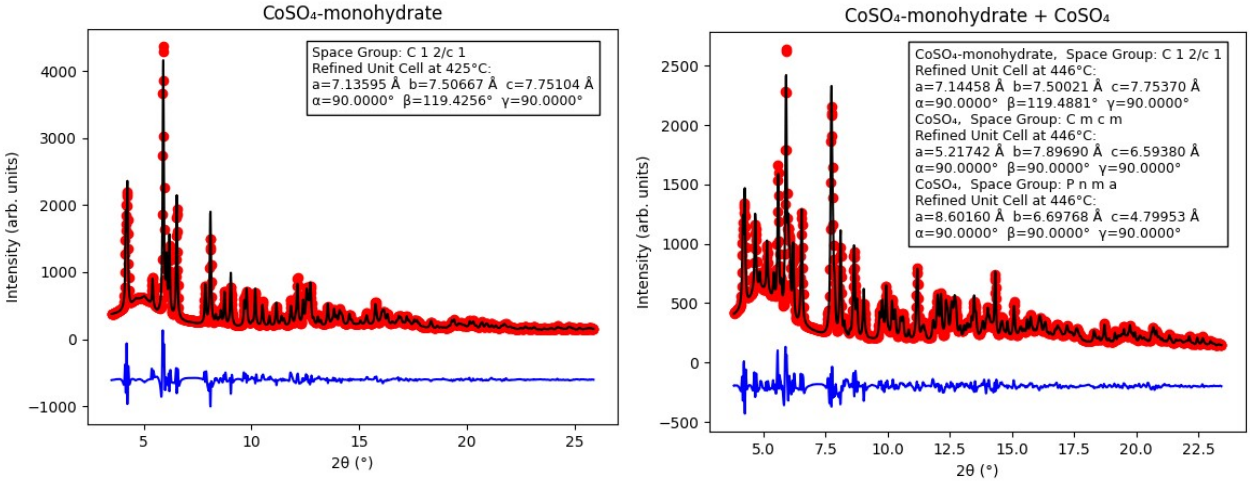

S5.25 $Cu(acac)_2$ in water

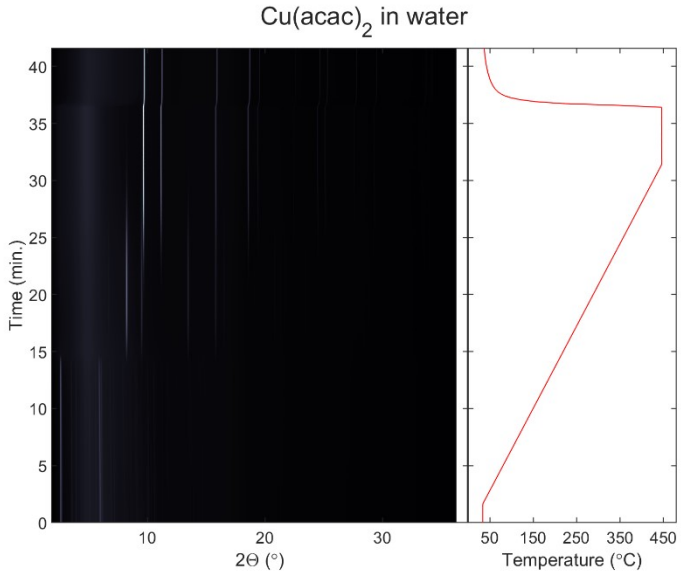
Cu(acac)2 in water
Time (min.)
2Θ (°)
Temperature (°C)

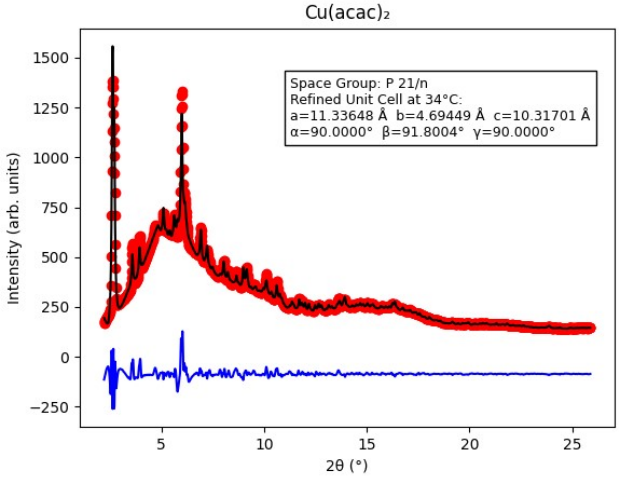
Cu(acac)₂
Space Group: P 21/n
Refined Unit Cell at 34°C:
a=11.33648 Å b=4.69449 Å c=10.31701 Å
α=90.0000° β=91.8004° γ=90.0000°
Intensity (arb. units)
2θ (°)

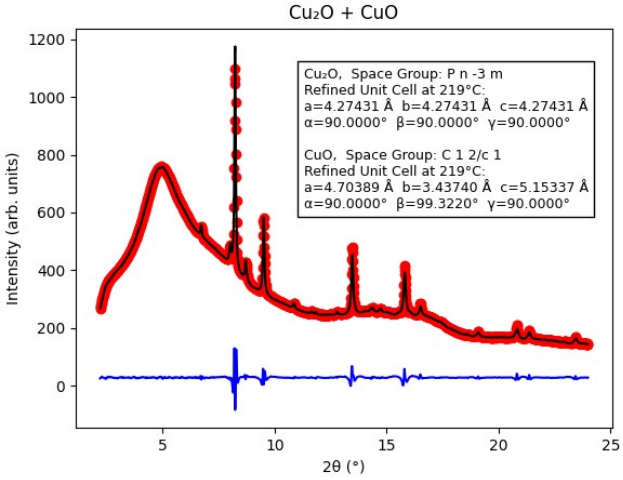
Cu₂O + CuO
Cu₂O, Space Group: P n -3 m
Refined Unit Cell at 219°C:
a=4.27431 Å b=4.27431 Å c=4.27431 Å
α=90.0000° β=90.0000° γ=90.0000°
CuO, Space Group: C 1 2/c 1
Refined Unit Cell at 219°C:
a=4.70389 Å b=3.43740 Å c=5.15337 Å
α=90.0000° β=99.3220° γ=90.0000°
Intensity (arb. units)
2θ (°)

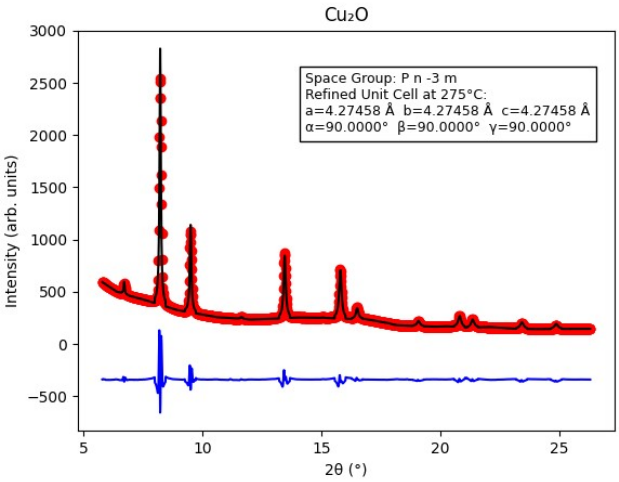
Cu₂O
Space Group: P n -3 m
Refined Unit Cell at 275°C:
a=4.27458 Å b=4.27458 Å c=4.27458 Å
α=90.0000° β=90.0000° γ=90.0000°
Intensity (arb. units)
2θ (°)

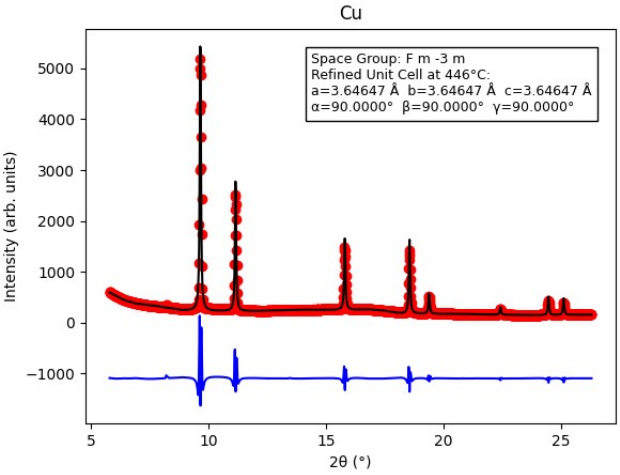
Cu
Space Group: F m -3 m
Refined Unit Cell at 446°C:
a=3.64647 Å b=3.64647 Å c=3.64647 Å
α=90.0000° β=90.0000° γ=90.0000°
Intensity (arb. units)
2θ (°)

S5.26 $Cu(ace)_2 \cdot H_2O$ in water

The mineral name of the initial phase, $Cu(ace)_2 \cdot ½H_2O$, is hooganite. For Cu_2O and Cu, intense peaks from single crystals caused unreliable relative intensities between reflections and between subsequent diffractograms.

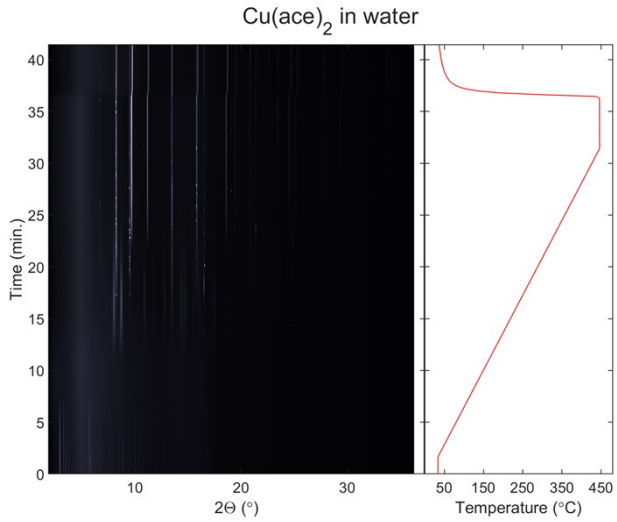

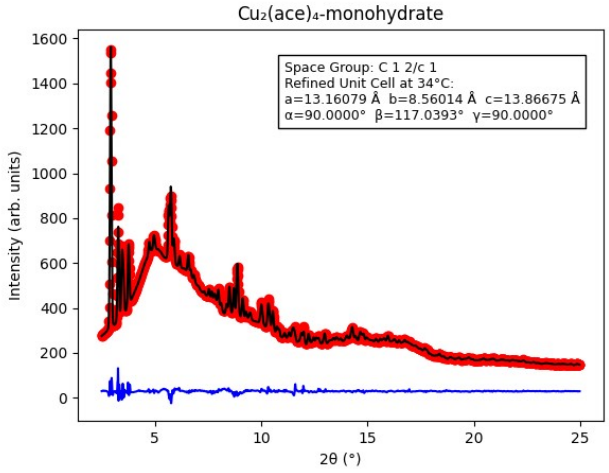

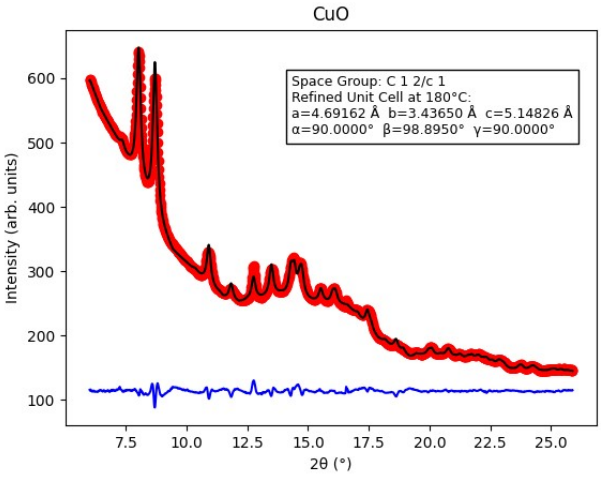

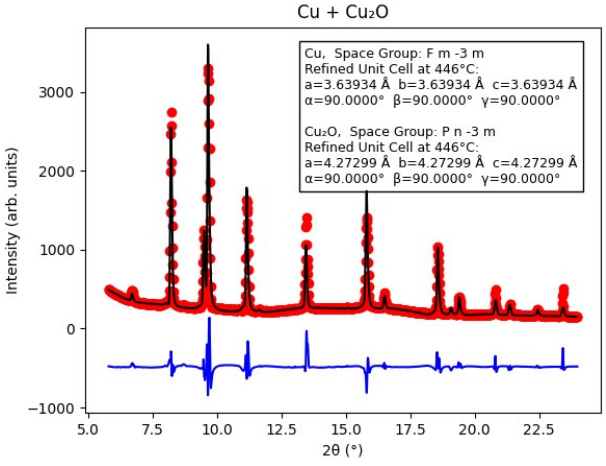

S5.27 $CuCl_2 \cdot 2H_2O$ in water

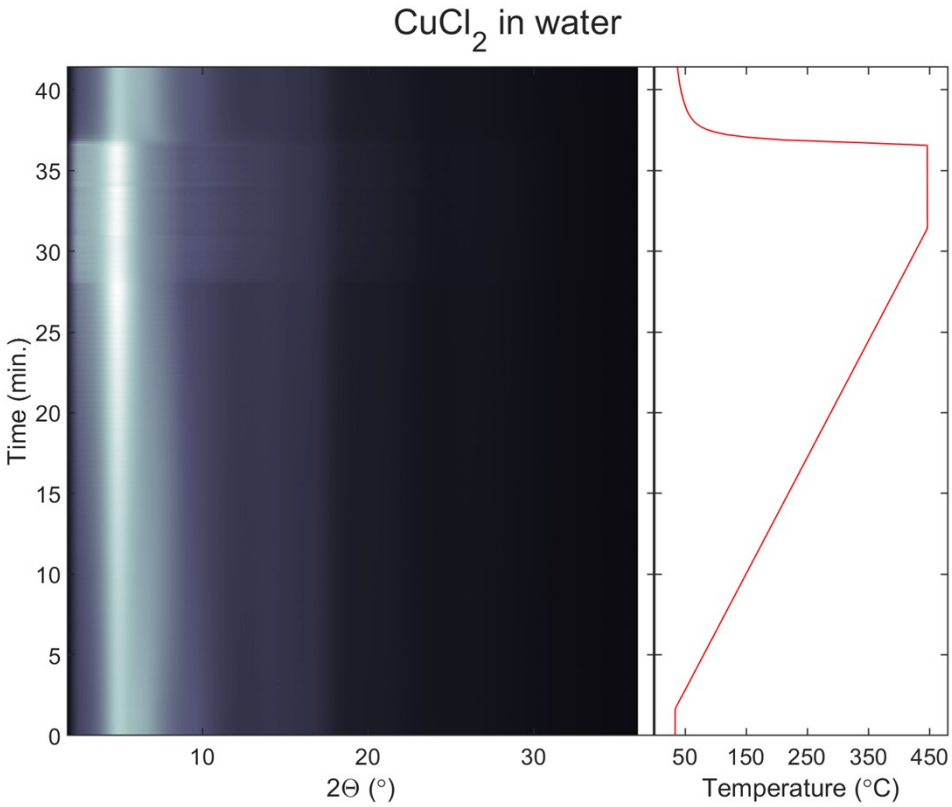

S5.28 CuI in water

At high temperature, intense peaks from single crystals caused unreliable relative intensities between reflections and between subsequent diffractograms.

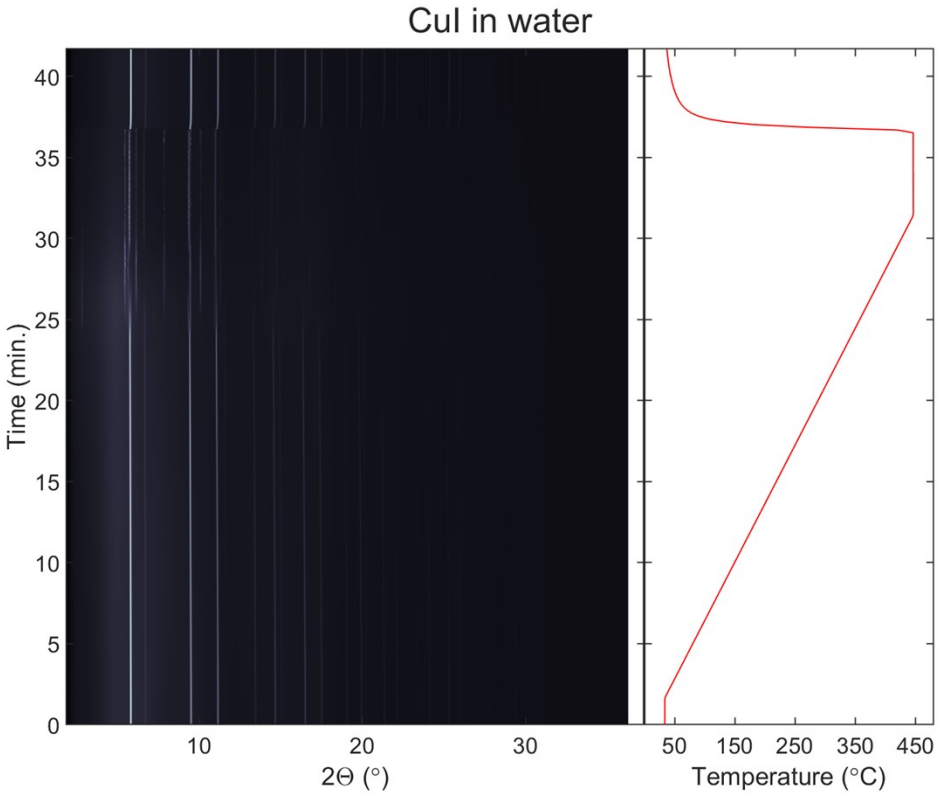

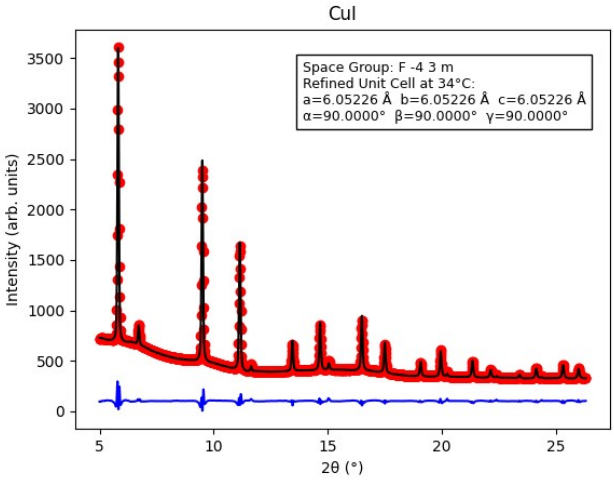

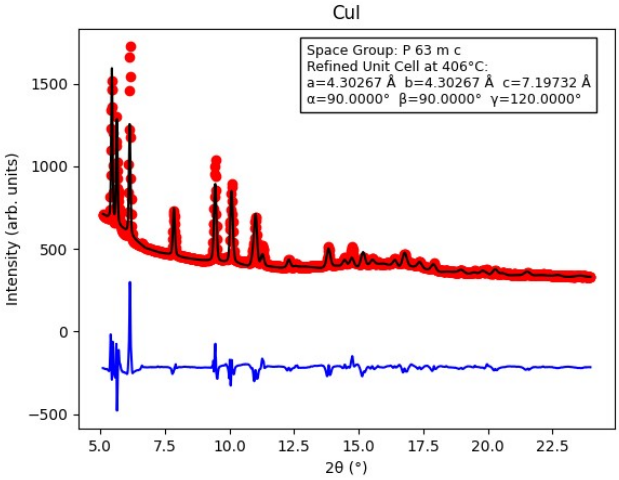

S5.29 $Cu(NO_3)_2 \cdot 3H_2O$ in water

Intense peaks from single crystals caused unreliable relative intensities between reflections and between subsequent diffractograms.

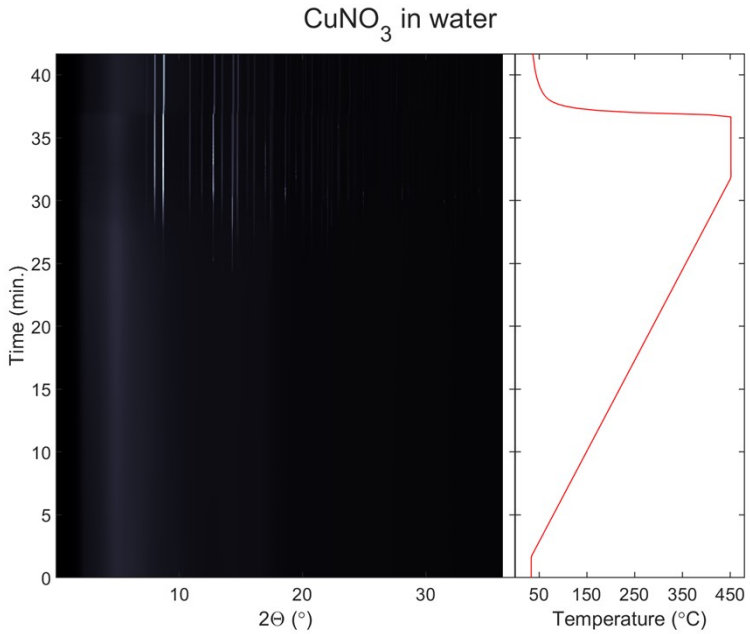

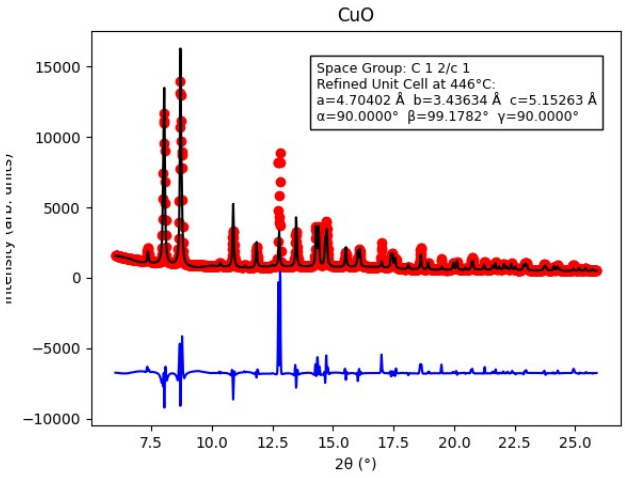

S5.30 $CuSO_4 \cdot 6H_2O$ in water

Intense peaks from single crystals caused unreliable relative intensities between reflections and between subsequent diffractograms.

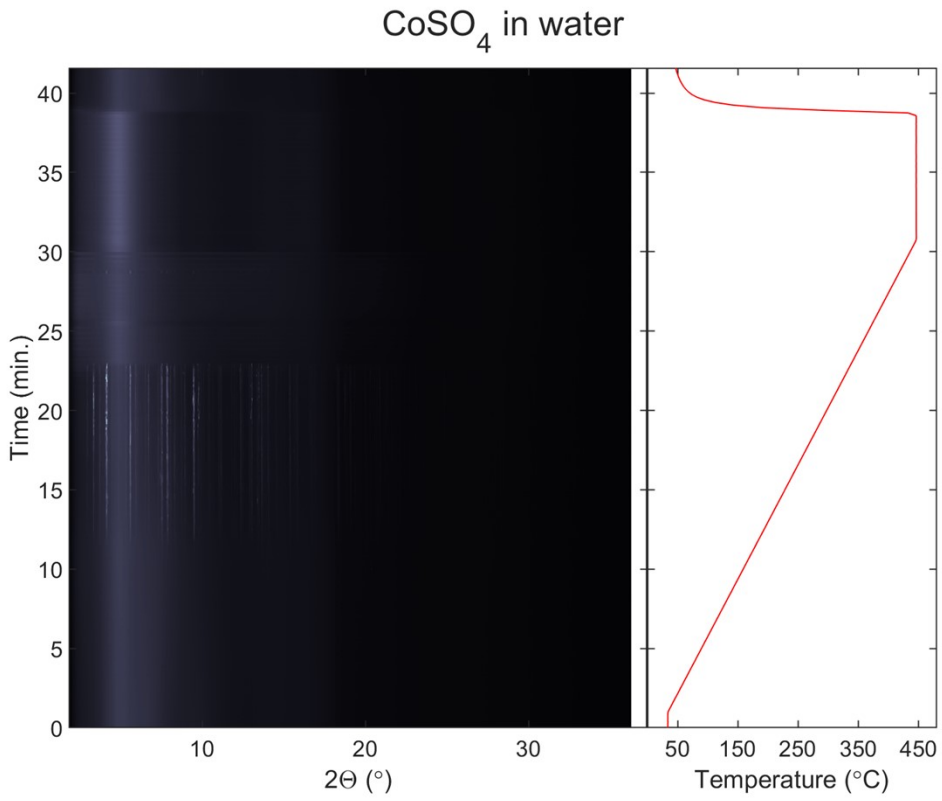

S5.31 $Mn(acac)_2$ in water

The refinement of Mn_2SiO_4 was challenged by poor background description in 2θ regions with many overlapping peaks but modelled all positions of reflections.

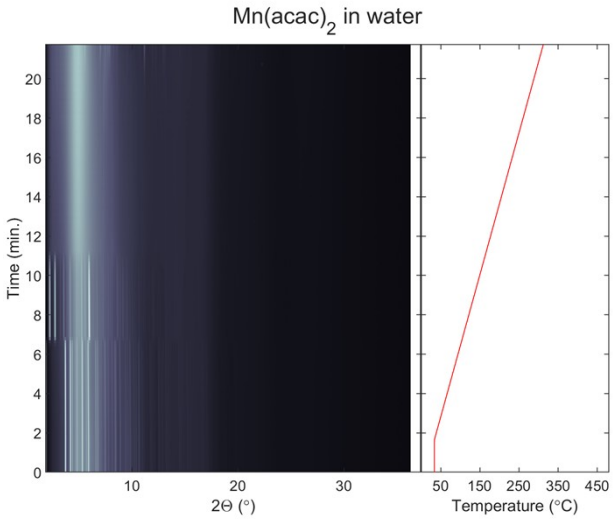

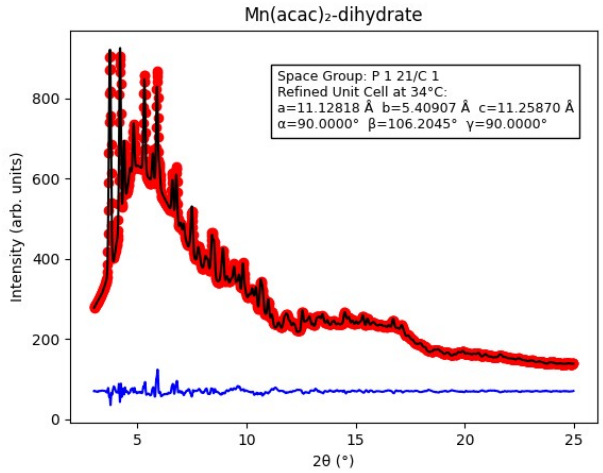

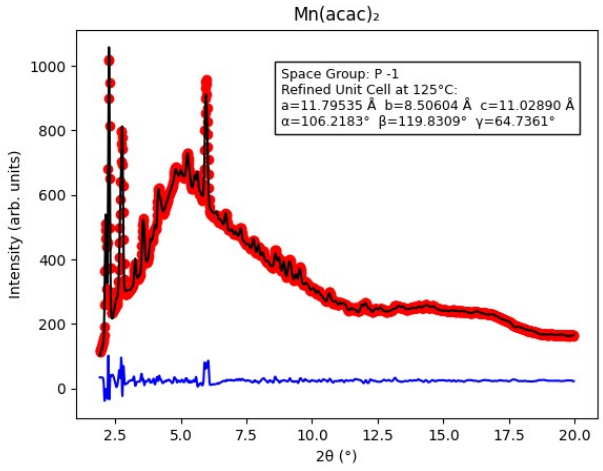

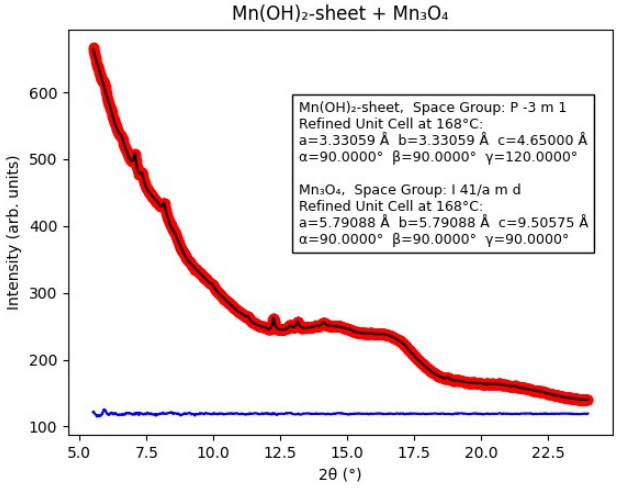

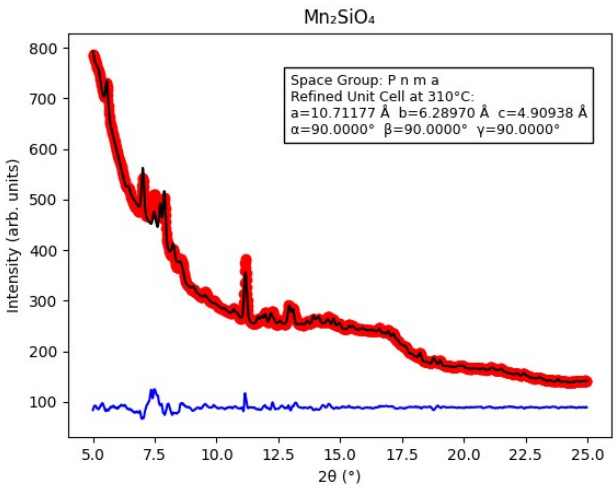

S5.32 $Mn(ace)_2 \cdot 4H_2O$ in water

The refinement of Mn_2SiO_4 was challenged by poor background description in 2θ regions with many

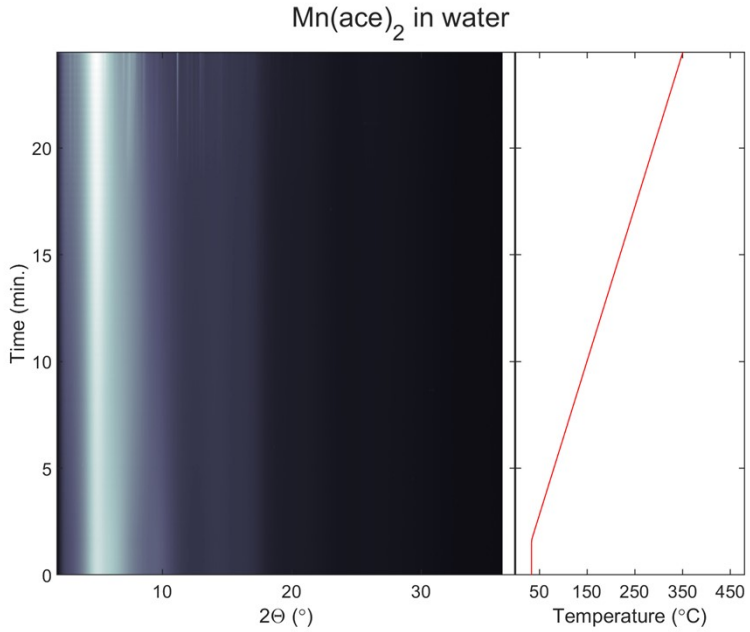

overlapping peaks but modelled all positions of reflections.

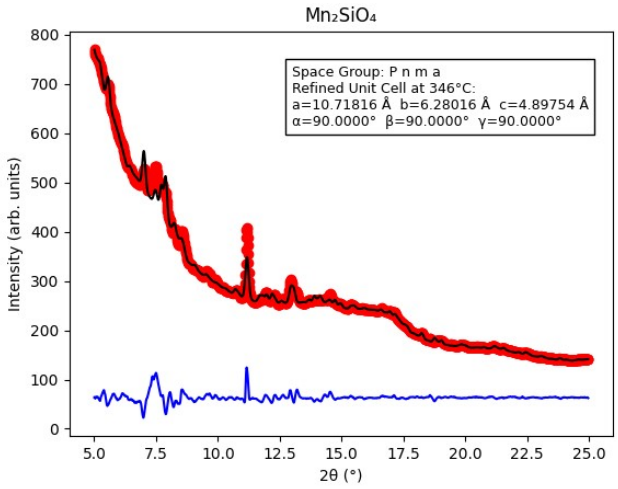

S5.33 $MnCl_2 \cdot H_2O$ in water

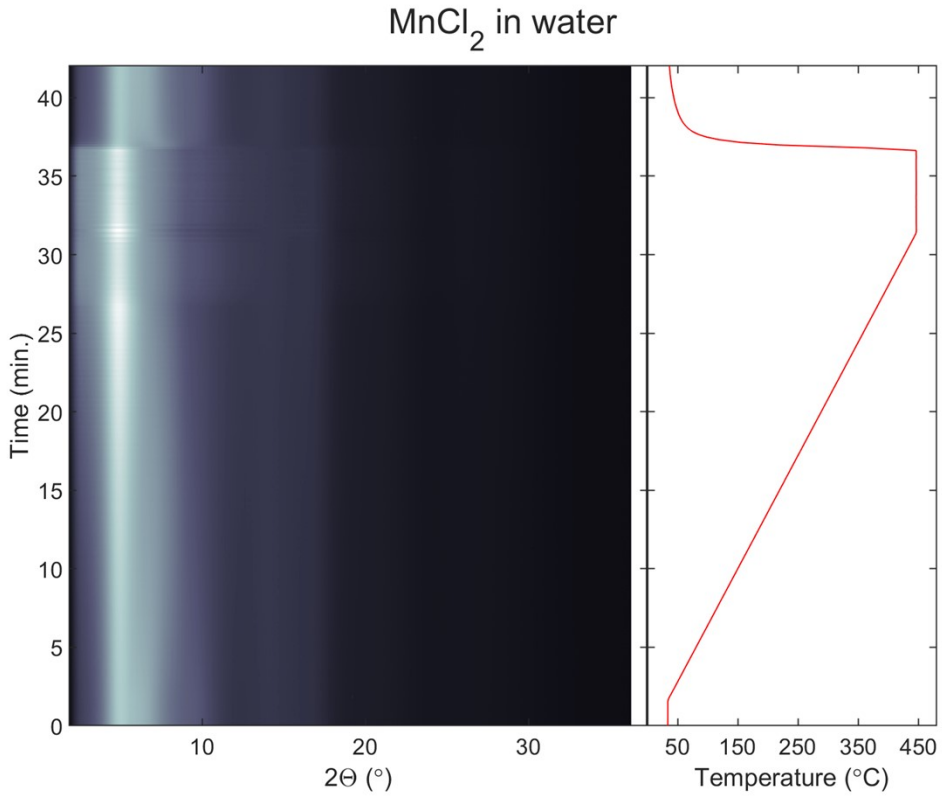

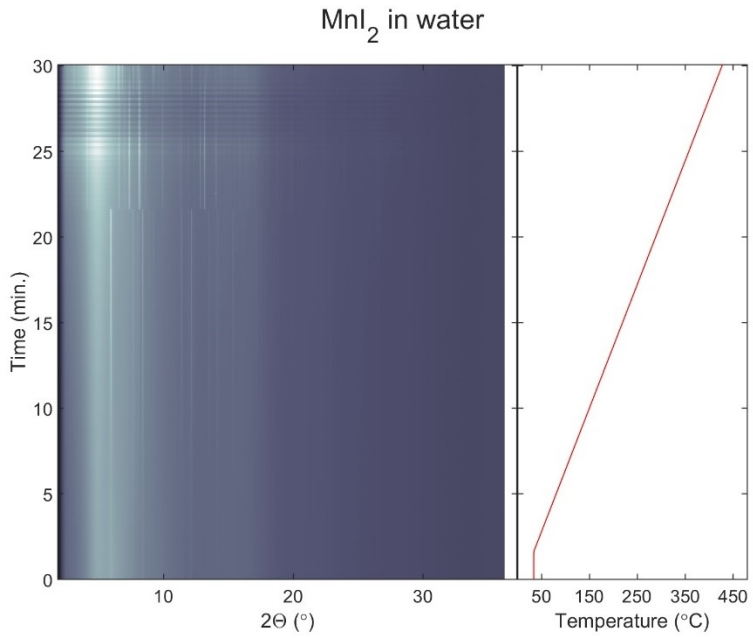

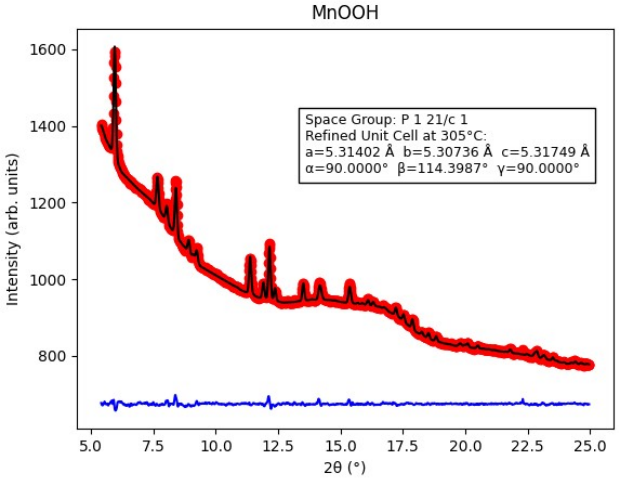

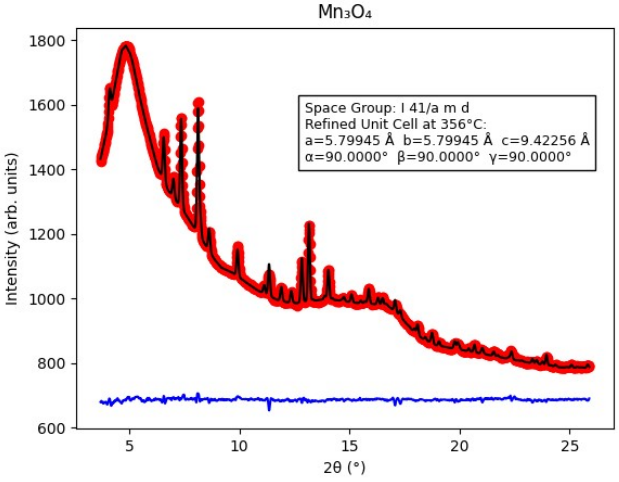

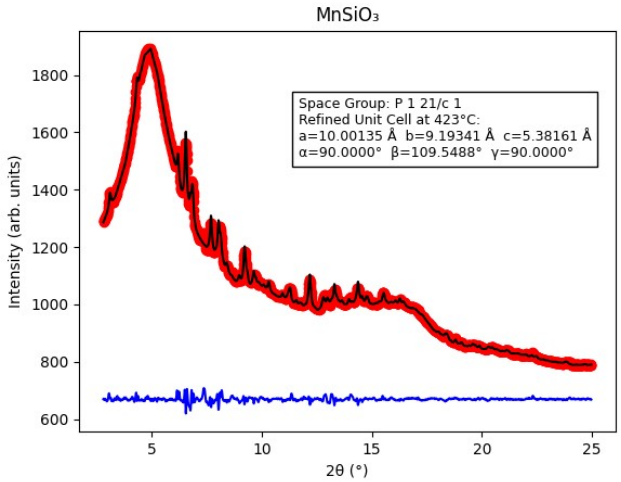

S5.34 MnI_2 in water

S5.35 $Mn(NO_3)_2 \cdot 4H_2O$ in water

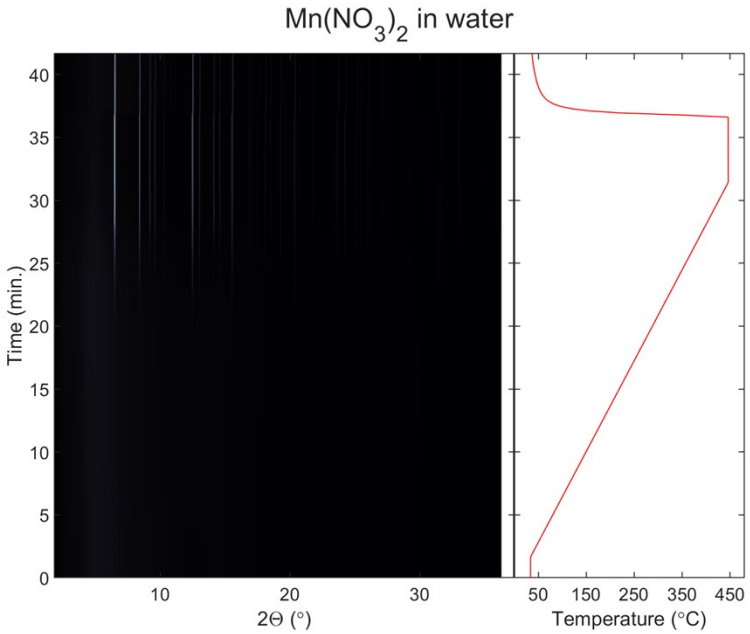

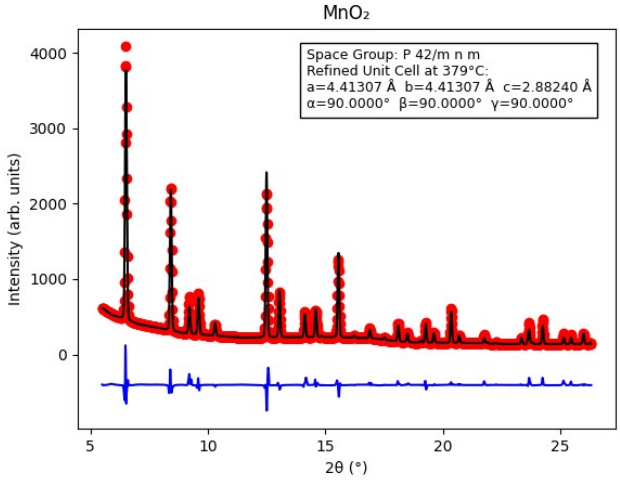

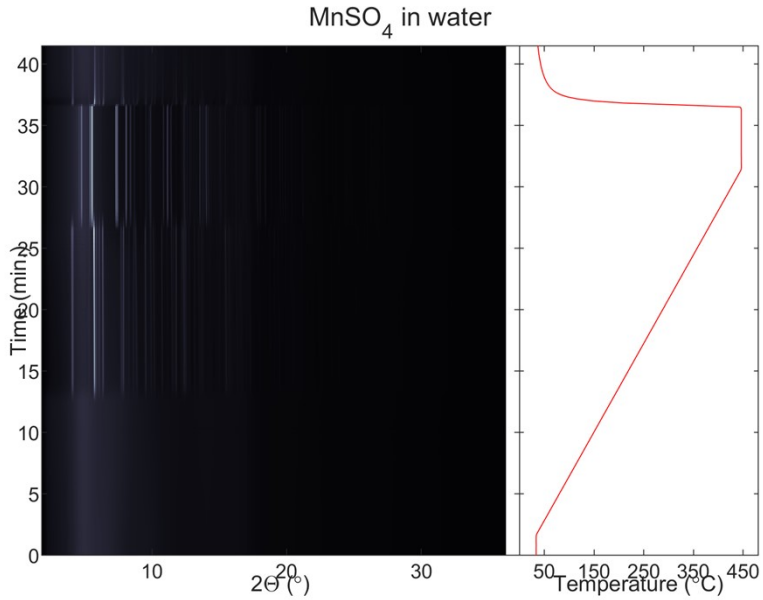

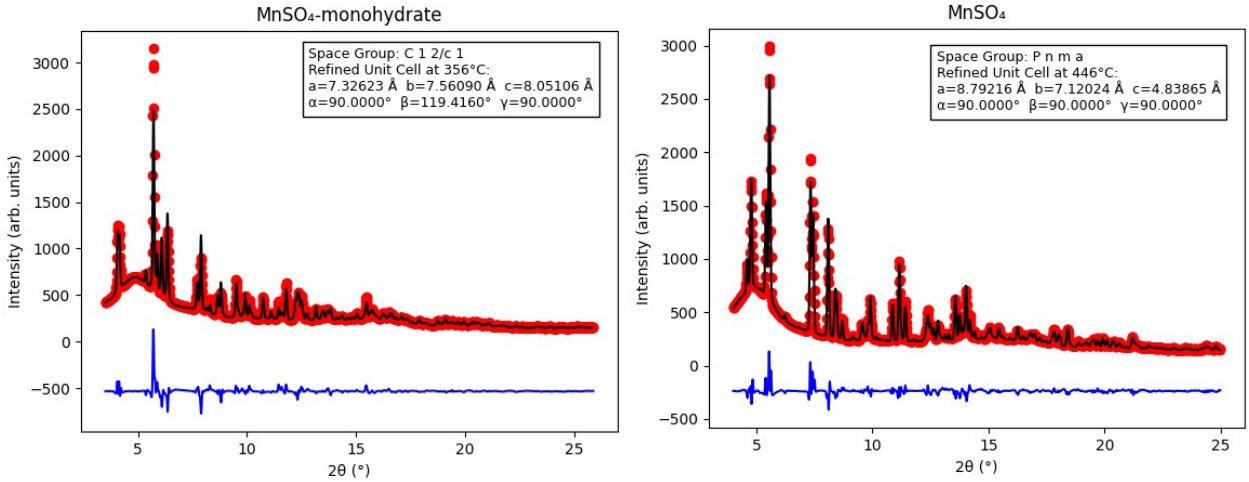

S5.36 $MnSO_4 \cdot H_2O$ in water